

X-550-69-277
PREPRINT

NASA TM X- 63636

APOLLO 6, 7, AND 8 BLACKOUT TEST RESULTS

JOHN W. MARINI
FREDERICK W. HAGER

JULY 1969



**GODDARD SPACE FLIGHT CENTER
GREENBELT, MARYLAND**

N69-6249

FACILITY FORM 602

(ACCESSION NUMBER)	(THRU)
32	1
(PAGES)	(CODE)
TMX-63636	07
(NASA CR OR TMX OR AD NUMBER)	(CATEGORY)

X-550-69-277
PREPRINT

APOLLO 6, 7, AND 8
BLACKOUT TEST RESULTS

John W. Marini
Frederick W. Hager*

JULY 1969

* Bendix Employee under contract to GSFC, Contract Number NAS5-10750.

Goddard Space Flight Center
Greenbelt, Maryland

APOLLO 6, 7, AND 8
BLACKOUT TEST RESULTS

John W. Marini
Frederick W. Hager

ABSTRACT

S-band communication blackout measurements made during the reentry phases of the Apollo 6, 7, and 8 missions are presented. The occurrence of blackout as a function of the altitude and speed of the reentering Apollo Command Module are compared with a theoretical curve. The agreement is good at the high speed end of the curve, but poor for the one point available at the low speed end.

PRECEDING PAGE BLANK NOT FILMED.

CONTENTS

	<u>Page</u>
I. INTRODUCTION	1
II. APOLLO-6 REENTRY	1
A. NASA 427 Data	1
B. "Watertown" Data	2
C. Results	2
III. APOLLO-7 REENTRY	3
A. MIL, GBM and NASA 427 Anomalous Loss of Signal	3
B. ARIA 5 Data	4
C. Results	4
IV. APOLLO-8 REENTRY	4
A. ARIA 1 Data	7
B. Results	7
V. CONCLUSIONS	7
REFERENCES	8

~~CONFIDENTIAL~~

APOLLO 6, 7, AND 8 BLACKOUT TEST RESULTS

I. INTRODUCTION

This report contains the results of S-band (2287.5 MHz) blackout (Reference 1) measurements taken during the reentry phases of the Apollo 6, 7, and 8 missions. The measurements of the occurrence of blackout are compared with a theoretical prediction curve developed at the Cornell Aeronautical Laboratory (Reference 2).

II. APOLLO-6 REENTRY

Apollo-6 was launched on April 4, 1968, at 12:00:01 GMT (Reference 3). The mission was non-nominal. Because of S-II engine malfunctions, reentry took place about 600 nautical miles downrange of the planned position and at a lower speed. The Command Module splashed down in the Pacific Ocean at 21 hours, 57 minutes, GMT, not quite 10 hours after lift-off.

A ground track of the reentry trajectory is shown in Figure 1. Reentry (400,000 ft. altitude) occurred at 21 hours, 28 minutes, 29 seconds, GMT. Blackout (loss of signal because of the reentry plasma sheath) was observed by both the NASA 427 instrumented aircraft and the Apollo reentry ship "Watertown" 25 seconds after reentry. The NASA 427 Aircraft was flying at an altitude of about 6,000 feet at the position shown in Figure 1, Latitude $31^{\circ} 05'N$ and Longitude $168^{\circ} 55'E$ at the time of blackout. The "Watertown" was located at $30^{\circ} 36'N$ Latitude and $156^{\circ} 30'E$ Longitude.

A. NASA 427 Data

The NASA 427 instrumented aircraft was based at Wake Island. The aircraft was equipped with a manually-steered S-band dish antenna and a calibrated S-band receiver. A recording of the signal strength from the reentering Command Module at the time of S-band blackout is shown in Figure 2. The deterioration of signal strength is abrupt, and appears to begin less than one second before complete loss of signal. The change was about 10 dB when the Command Module had descended to 323,600 feet altitude. The speed of the Module was 31,600 feet per second at this time.

During the data stretch shown, the operator of the receiving dish aboard the NASA 427 was able to maintain the pointing angles to within about 3 degrees as shown in Figure 3. Since the 3 dB beamwidth of the antenna was ± 4 degrees (Reference 4), receiving antenna pointing errors contributed less than 3 dB to the change of signal strength in Figure 2.

The slant range from the aircraft to the Command Module did not vary significantly during the period of signal decay. The range was 111.8 nautical miles at 21:38:53 and 111.1 nautical miles at 21:38:54, so the change in signal strength caused by change in range was negligible.

The elevation angle of the Command Module as seen from the NASA 427 remained at approximately 27 degrees during the same time period. At this elevation, a wave transmitted from the Command Module and reflected from the surface of the ocean would arrive far outside of the main beam of the receiving antenna. Multipath from this source, therefore, was not significant.

The S-band antenna system on the Command Module consists of four cavity-backed right-hand circularly-polarized helices (Figure 4). Of these four, only pair B (antennas 2 and 4 connected in parallel) was transmitting at the time of blackout. In Figure 5, the antenna pattern of this pair (Reproduced from Reference 5) together with the polar coordinates of the NASA 427 aircraft plotted at one-second intervals about the time of blackout are shown. The gain function of the transmitting antennas was constant to within 1 dB from 21:38:51 to 21:38:55, and therefore did not contribute appreciably to the measured change in signal strength.

The calculation of the elevation and polar angles was made (Reference 6) using a reentry trajectory provided by the Data Processing Branch, Computation and Analysis Division of the Manned Spacecraft Center.

B. "Watertown" Data

The NASA reentry ship "Watertown" locked on to the spacecraft S-band transponder some time before reentry, and maintained lock until loss of signal. A copy of the strip chart recording of the received signal is shown in Figure 6. The time of blackout agrees with that observed on the NASA 427.

C. Results

The reentry trajectory of the Apollo-6 Command Module is plotted on an altitude-speed diagram in Figure 7. The blackout point obtained by the NASA 427,

323,600 feet altitude at 31,600 feet per second, appears to be a valid one, as the decrease in signal strength observed was not caused by either transmitting antenna gain changes, receiving antenna pointing errors or multipath. However, in this type of field measurement there is always some small possibility that the observed decrease could have been caused by some other effect not taken into consideration. In any case, the point does represent the lowest altitude at which an S-band signal has been received from the Apollo Command Module traveling at a speed of 31,600 feet per second, and as such, is an upper bound of the blackout prediction curve.

III. APOLLO-7 REENTRY

The Apollo-7 Command Module reentered and splashed down in the Atlantic Ocean on October 22, 1968. The reentry ground track is shown in Figure 8. S-band signals from the Command Module were monitored by the Unified S-Band Stations TEX, MIL, and GBM at Corpus Christi, Merritt Island and Grand Bahama Island, respectively. In addition, signals were received by the NASA 427 instrumented aircraft flying at about 6,000 feet altitude at 28°N and $81^{\circ} 35'\text{W}$ near Lakeland, Florida, and by the ARIA 5 aircraft flying at about 35,000 feet altitude at $28^{\circ} 10'\text{N}$ and 89°W over the Gulf of Mexico.

A. MIL, GBM and NASA 427 Anomalous Loss of Signal

AGC recordings of the loss of signal by NASA 427, MIL, and GBM are shown in Figures 9, 10 and 11, respectively. As nearly as can be determined from these recordings, the dip in signal strength is simultaneous for the three stations. MIL was locked on to the spacecraft transponder at that time, and the telemetry recording of the strength of the signal received from MIL by the spacecraft transponder shows a simultaneous decrease in signal strength also. These data would all be consistent with signal blackout caused by the formation of an overdense plasma sheath except for two considerations. First, the altitude of the Command Module was too high, in view of the existing speed, for the formation of a sheath of sufficient electrical density to effect S-band signals. Second, the ARIA 5 aircraft, which viewed the Command Module at a markedly different aspect, observed a dip in signal strength at that time, but did not lose the signal.

The ARIA 5 AGC record for the time in question is shown in Figure 12. A momentary dip in signal strength of about 17 dB took place at about 10:57:39 GMT, but the ARIA continued to track the signal past this point. It is interesting to note that the decrease occurred at slightly different times for the right-hand circular (RHC) and the left-hand circular (LHC) polarizations of the receiving antennas used. In spite of the coincidence in time, however, it is not certain that the dip seen by ARIA 5 and the loss of signal at MIL, GBM and NASA 427

arose from the same source, especially in view of the unsteady appearance of the ARIA 5 AGC record in the time following the anomaly.

In Figure 13 is shown the data from TEX which likewise continued to track beyond 10:57:39, and apparently lost signal because of loss of pointing information as the Command Module disappeared over the horizon.

The geometrical elevation angles of the Command Module as seen from the various stations are given in Table I. Also given in Table I are the values of transmitting antenna gain in decibels below a reference level of 4 dB. These values were obtained from the gain function plot of Figure 14.

The traces in Figure 14 corresponding to MIL, GBM and the NASA 427 all pass near a large hole in the antenna pattern, centered at about $\phi = 135^\circ$, $\theta = 90^\circ$ on the side of the spacecraft opposite to the radiating antenna. It is conceivable that either the calculated location of the traces or the ground-measured pattern did not correspond exactly to the actual in-flight situation, and that the loss of signal was caused by the null in the antenna pattern.

B. ARIA 5 Data

The ARIA 5 aircraft continued to receive a S-band signal long after MIL, GBM and NASA 427 had lost theirs. The signal (Figure 15) became noisy at 10:58:40 GMT and was lost at 10:59:30. The noisy signal is typical of multi-path effects occurring at low elevation angles (Table II), and the loss of signal can be attributed to the passing of the Command Module over the radio horizon. Thus, the ARIA 5 data exhibits no positive evidence of plasma-sheath induced communication blackout at all.

C. Results

Figure 16 is the altitude-speed diagram of Apollo-7 reentry. The loss of signal by NASA 427, MIL, and GBM occurred when the Command Module was at an altitude of 319,000 feet and traveling at a speed of 24,600 feet per second. ARIA 5 did not lose signal until the Module had descended to 228,000 feet when its speed was 24,000 feet per second. Blackout attributable to plasma sheath effects was not observed.

IV. APOLLO-8 REENTRY

The Apollo-8 mission, the first manned lunar orbital flight, lasted 6 days. The Command Module splashed down in the Pacific Ocean on December 27, 1968, at 15 hours, 50 minutes, GMT. The reentry ground track is shown in Figure 17.

Table I
Antenna Gain and Elevation of the Command Module, Apollo 7 Reentry

Time	NASA 427		MIL		GBM		ARIA 5		TEX	
	dB	Degree	dB	Degree	dB	Degree	dB	Degree	dB	Degree
10:57:00	20	4.55	24	3.79	15	0.49	14	24.44	9	3.21
10:57:02	18	4.72	17	3.95	14	0.59	13	24.19	9	3.0
10:57:04	17	4.89	20	4.11	14	0.70	12	23.84	9	2.79
10:57:06	16	5.07	20	4.28	14	0.81	12	23.38	9	2.59
10:57:08	16	5.26	20	4.45	15	0.91	11	22.83	7	2.39
10:57:10	15	5.45	21	4.62	15	1.02	10	22.20	7	2.19
10:57:12	16	5.64	21	4.80	14	1.13	10	21.52	8	2.00
10:57:14	14	5.84	29	4.98	14	1.24	10	20.79	8	1.80
10:57:16	12	6.04	29	5.17	14	1.35	10	20.04	8	1.62
10:57:18	13	6.25	25	5.36	14	1.47	10	19.26	8	1.44
10:57:20	13	6.47	25	5.56	14	1.58	10	18.48	8	1.26
10:57:22	13	6.69	24	5.76	14	1.70	11	17.71	8	1.09
10:57:24	14	6.92	25	5.97	18	1.81	12	16.95	8	0.91
10:57:26	14	7.15	24	6.19	19	1.93	11	16.20	7	0.74
10:57:28	14	7.39	24	6.41	19	2.05	12	15.48	7	0.58
10:57:30	14	7.64	24	6.64	19	2.17	12	14.77	7	0.41
10:57:32	13	7.90	23	6.87	19	2.30	12	14.09	8	0.25
10:57:34	13	8.17	20	7.12	18	2.42	12	13.44	9	0.09
10:57:36	13	8.45	22	7.37	14	2.54	13	12.81	9	-0.07
10:57:38	13	8.73	20	7.63	13	2.67	13	12.21	9	-0.22
*10:57:40	18	9.03	20	7.91	12	2.80	12	11.63	9	-0.38
10:57:42	19	9.3	15	8.19	12	2.93	12	11.08	9	-0.53
10:57:44	20	9.66	15	8.48	13	3.06	12	10.55	9	-0.68
10:57:46	18	9.99	14	8.79	14	3.20	11	10.05	9	-0.82
10:57:48	19	10.33	14	9.11	15	3.33	11	9.56	9	-0.97
10:57:50	18	10.69	14	9.43	16	3.47	11	9.10	9	-1.11
10:57:52	15	11.06	20	9.79	16	3.61	11	8.66	8	-1.25
10:57:54	13	11.45	20	10.15	19	3.76	12	8.23	8	-1.39
10:57:56	13	11.85	19	10.53	19	3.90	11	7.82	8	-1.53
10:57:58	11	12.27	18	10.93	18	4.05	11	7.43	8	-1.66
10:58:00	11	12.70	16	11.36	17	4.20	12	7.06	8	-1.80
10:58:02	12	13.15	12	11.80	20	4.35	12	6.70	8	-1.93
10:58:04	12	13.61	12	12.27	19	4.50	12	6.35	9	-2.07
10:58:06	11	14.09	12	12.76	18	4.66	12	6.01	9	-2.19
10:58:08	12	14.58	12	13.28	18	4.82	12	5.69	9	-2.32
10:58:10	13	15.09	12	13.84	20	4.98	11	5.38	9	-2.45
10:58:12	13	15.60	12	14.42	21	5.15	11	5.08	9	-2.58
10:58:14	11	16.12	13	15.04	10	5.32	12	4.78	8	-2.70
10:58:16	11	16.15	10	15.70	14	5.49	10	4.50	8	-2.83
10:58:18	11	17.17	12	16.40	14	5.66	10	4.23	8	-2.95

*NASA 427, MIL, and GBM lost signal at this time.

Table II
Antenna Gain and Elevation of the Command Module in ARIA 5, APOLLO 7 Reentry

Time	Gain (dB)	Elevation Angle (Degree)
10:58:20	10	3.97
10:58:22	9	3.71
10:58:24	12	3.47
10:58:26	12	3.22
10:58:28	9	2.99
10:58:30	10	2.76
10:58:32	10	2.54
10:58:34	10	2.33
10:58:36	10	2.12
10:58:38	10	1.92
10:58:40	11	1.72
10:58:42	9	1.52
10:58:44	9	1.33
10:58:46	9	1.15
10:58:48	9	0.96
10:58:50	9	0.79
10:58:52	9	0.61
10:58:54	9	0.44
10:58:56	9	0.28
10:58:58	11	0.114
10:59:00	10	-0.045
10:59:02	10	-0.202
10:59:04	10	-0.356
10:59:06	10	-0.506
10:59:08	11	-0.65
10:59:10	11	-0.80
10:59:12	10	-0.94
10:59:14	13	-1.08
10:59:16	13	-1.22
10:59:18	12	-1.36
10:59:20	13	-1.49
10:59:22	12	-1.62
10:59:24	13	-1.75
10:59:26	13	-1.88
10:59:28	13	-2.00
10:59:30	13	-2.12

A. ARIA 1 Data

The ARIA 1 aircraft flying at $17^{\circ} 2'N$ latitude and $176^{\circ} 41'E$ longitude observed S-band blackout. The AGC record is shown in Figure 18. Loss of signal took place at about 15:37:37 GMT. This loss of signal was preceded by the slight ripple in the signal strength observed on another high-speed reentry (Reference 7).

The elevation angle of the Command Module with respect to ARIA 1 was about 11 degrees at the time of blackout. The gain of the transmitting antenna in the direction of ARIA 1, as shown in Figure 19, was not particularly favorable, but does not, nevertheless, appear to be the major cause of the change in signal strength.

B. Results

The altitude-speed plot of the Apollo-8 reentry is shown in Figure 20. ARIA 1 lost signal, apparently because of the reentry plasma sheath, when the Command Module was at an altitude of 329,000 feet and moving at a speed of 35,100 feet per second.

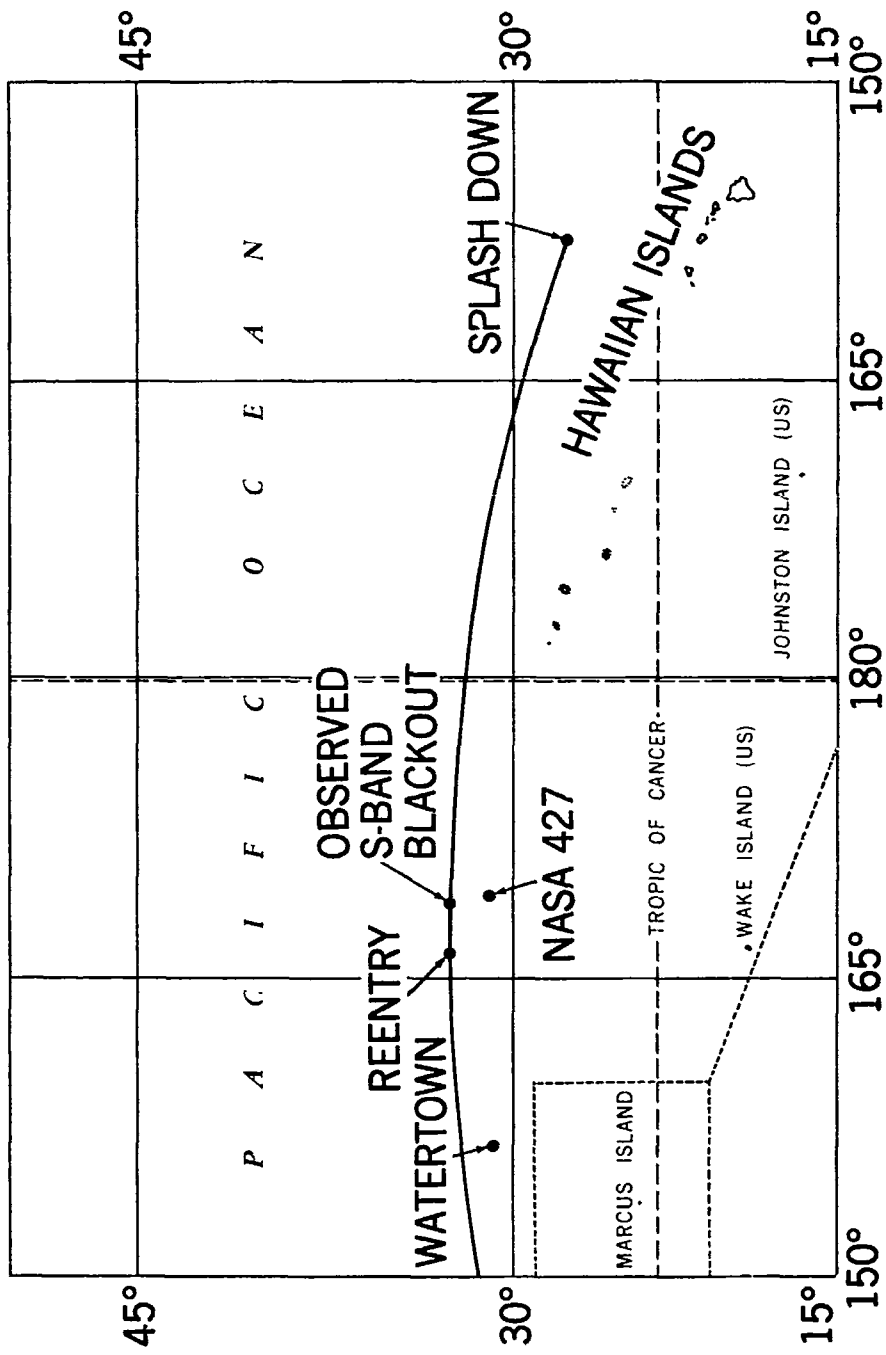
V. CONCLUSIONS

The blackout prediction curve from Reference 2, the points obtained on the Apollo missions 6, 7, and 8, and the point obtained on Apollo 4 mission (Reference 7) are plotted in Figure 21. S-band blackout should commence when the trajectory of the Apollo Command Module intersects the prediction curve, and trajectory points below the curve should be in blackout.

At the upper end of the curve, agreement with the points from Apollo 4, 6, and 8 is good. At the lower end, however, the curve should pass below the point obtained by ARIA 5 during Apollo 7 reentry. The discrepancy could conceivably have been caused by aspect angle differences. The ARIA 5 data was taken with the pointed end of the command module in view, while the blackout curve applies primarily to a broadside view of the module. In the absence of additional low-speed measurements, definite conclusions about agreement between blackout prediction and measured results cannot be made.

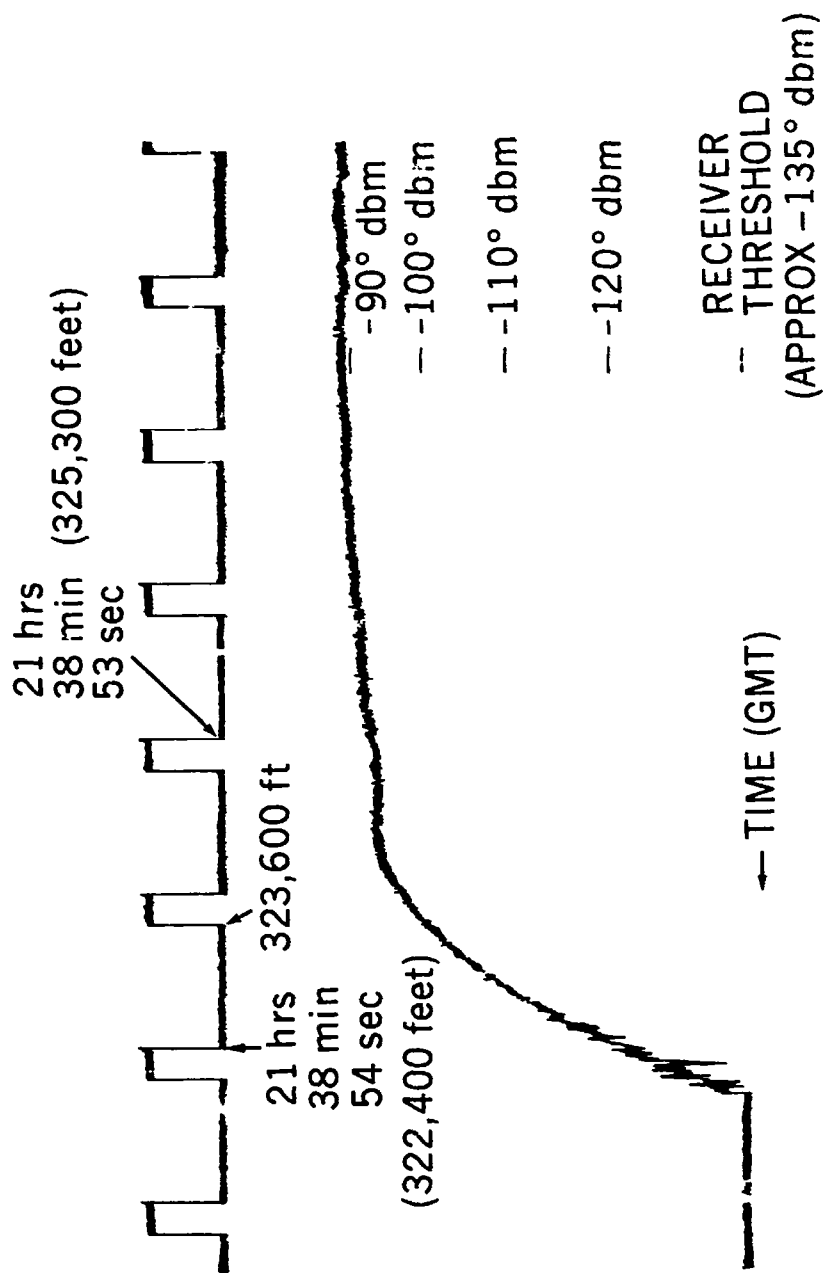
REFERENCES

1. R. Lehnert and B. Rosenbaum, "Plasma Effects on Apollo Reentry Communication," NASA TN D-2732, March 1965.
2. "Twelfth Quarterly Progress Report for Project Apollo," 1 October 1968 – 1 January 1969, prepared for GSFC by Cornell Aeronautical Laboratory, Inc. under Contract NAS 5-9978.
3. Manned Flight Planning and Analysis Division, "Performance Evaluation of the Unified S-Band Ground System for AS-502," GSFC X-834-68-241, June 1968.
4. J. Marini and W. Rice, "Reentry Test Plan for Apollo 6 (AS-502) GSFC X-551-68-64 Feb. 20, 1968.
5. J. F. Lindsey III, "Full Scale Block I Spacecraft 017 and 020 S-Band OMNI Antenna Patterns," MSC Internal Note No. 67-EE-14, June 1967.
6. F. W. Hager, "Apollo Reentry Acquisition and Radio Visibility Computer Program," GSFC X-551-68-500, Dec. 1968.
7. J. Marini, "Apollo 4 Blackout Test Results, Mares Island Entry," GSFC X-551-68-419, Nov. 1968.



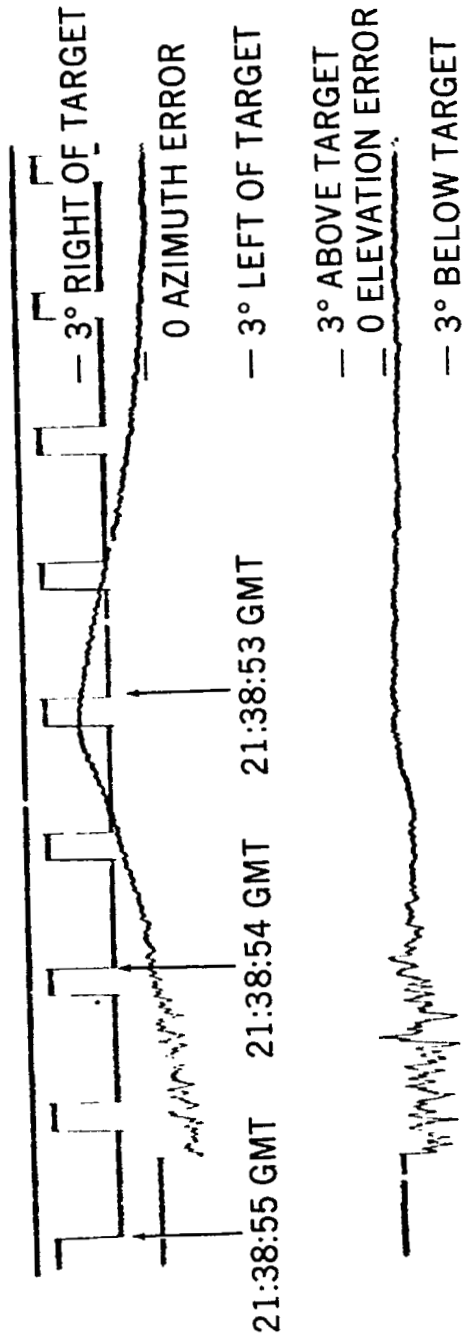
NASA-GSFC-T&DS
MISSION & TRAJECTORY ANALYSIS DIVISION
BRANCH 551 DATE 6-25-67
BY MARINI PLOT NO. 1167

Figure 1. Reentry Ground Track of Apollo 6



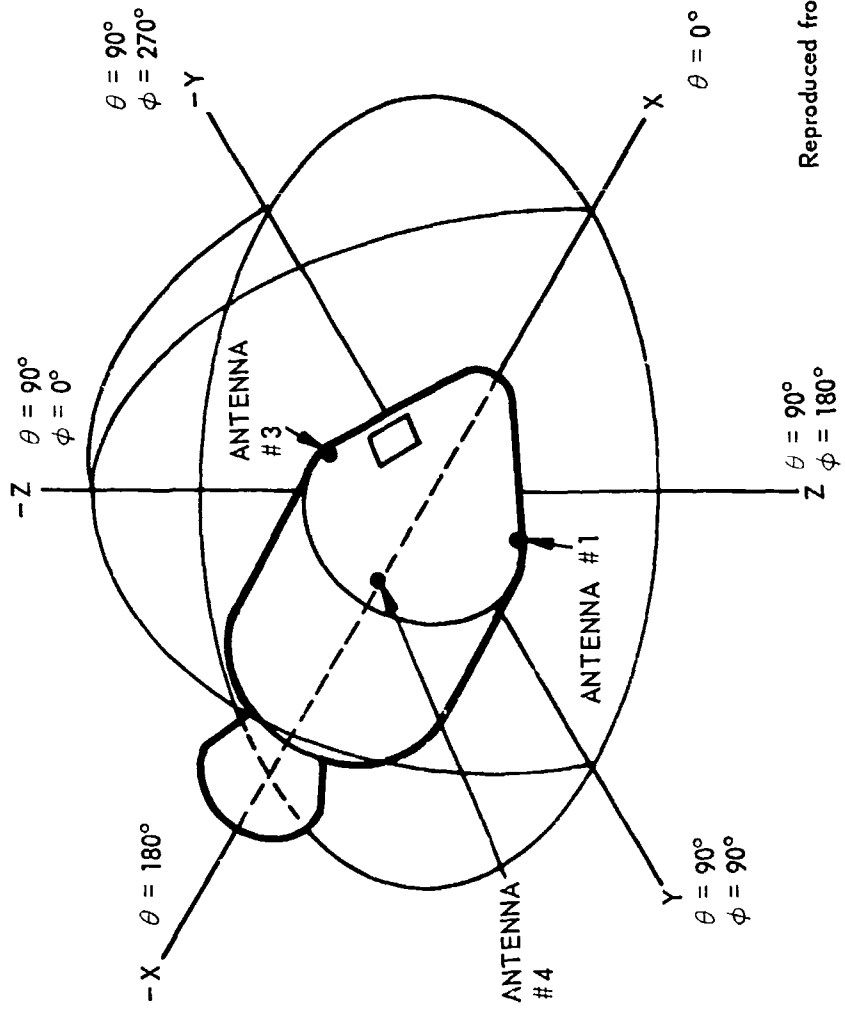
NASA-GSFC-T&DS
 MISSION & TRAJECTORY ANALYSIS DIVISION
 BRANCH MSAB DATE JUNE 17, 1969
 BY MARINI PLOT NO. 1168

Figure 2. Apollo 6 (AS-502) S-Band Signal Strength and Blackout, NASA 427



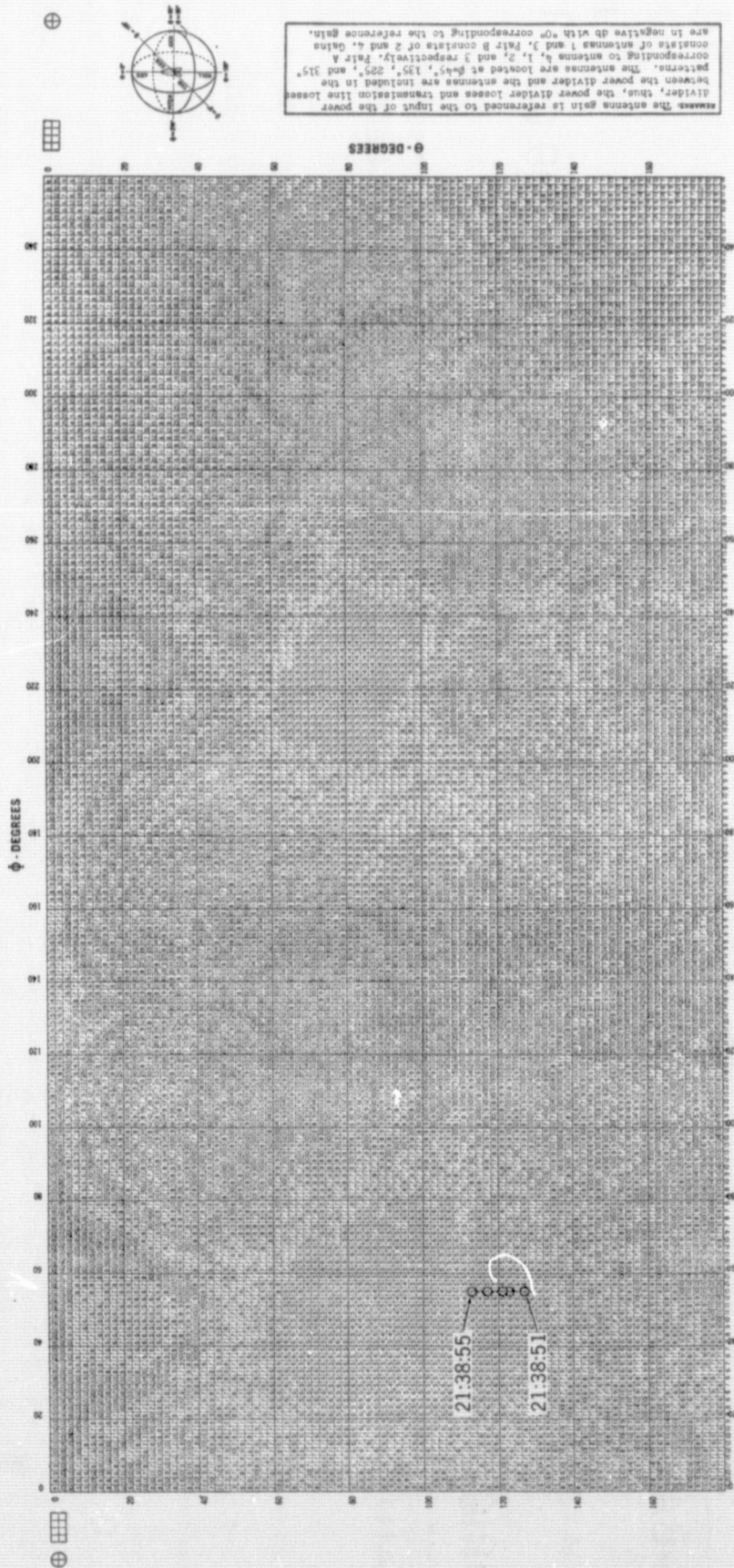
NASA-GSFC-T&DS
 MISSION & TRAJECTORY ANALYSIS DIVISION
 BRANCH MSAB DATE JUNE 17, 1969
 BY MARINI PLOT NO. 1169

Figure 3. NASA 427 Antenna Pointing Errors



Reproduced from Reference 4.

Figure 4. Antenna Coordinate System and Location of S-Band Helices



76

REMARKS: The antenna gain is referenced to the input of the power divider, thus, the power divider losses and transmission line losses between the antennas are included in the patterns. The antennas are located at $\theta = 45^\circ, 135^\circ, 225^\circ,$ and 315° corresponding to antennas 1, 2, 3, and 4 respectively. Pair A consists of antennas 1 and 3. Pair B consists of 2 and 4. Gains are in negative db with 0° corresponding to the reference gain.

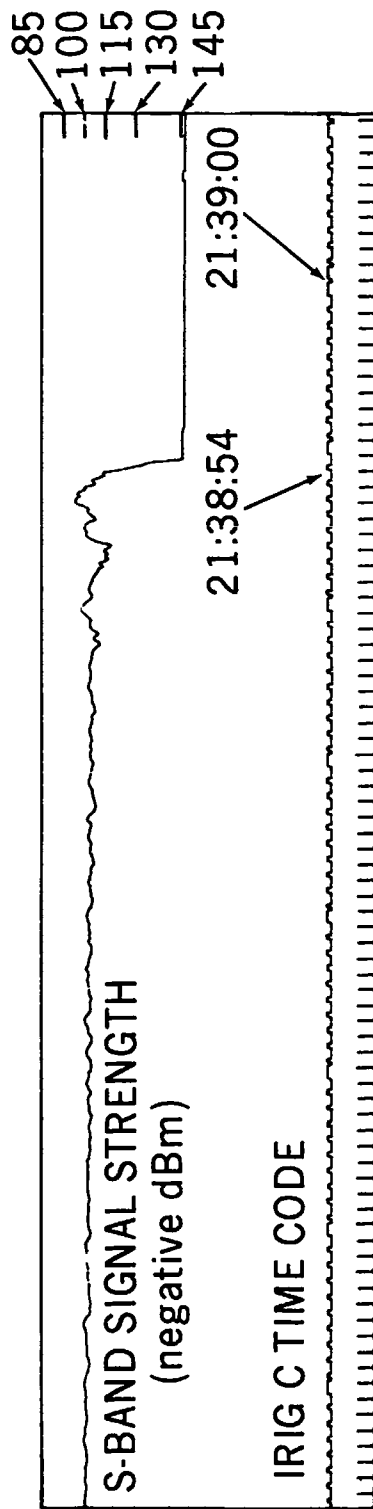
76

MISSION & TRAJECTORY ANALYSIS DIVISION
 BRANCH _____ DATE _____
 BY _____ PLOT NO. _____

TEST PROGRAM OR VEHICLE: SAC 017 and 020 DV
 DATE: 1-21-67
 ANTENNA NO: 76
 ORGANIZATION: ESO-528-Antenna Systems Section
 ENGINEER: J. L. HARRIS
 ANTENNA TYPE: Helixes 2 and 4 in parallel
 FEED: BNC, 5-ohm
 PATTERN MEASUREMENT FREQ: 2287.5 Mc
 PREDOMINANT POLARIZATION: Right Circular Helixes
 WORK SCALE: 0.11 LOCATION OF POINT P: B-A-B-17

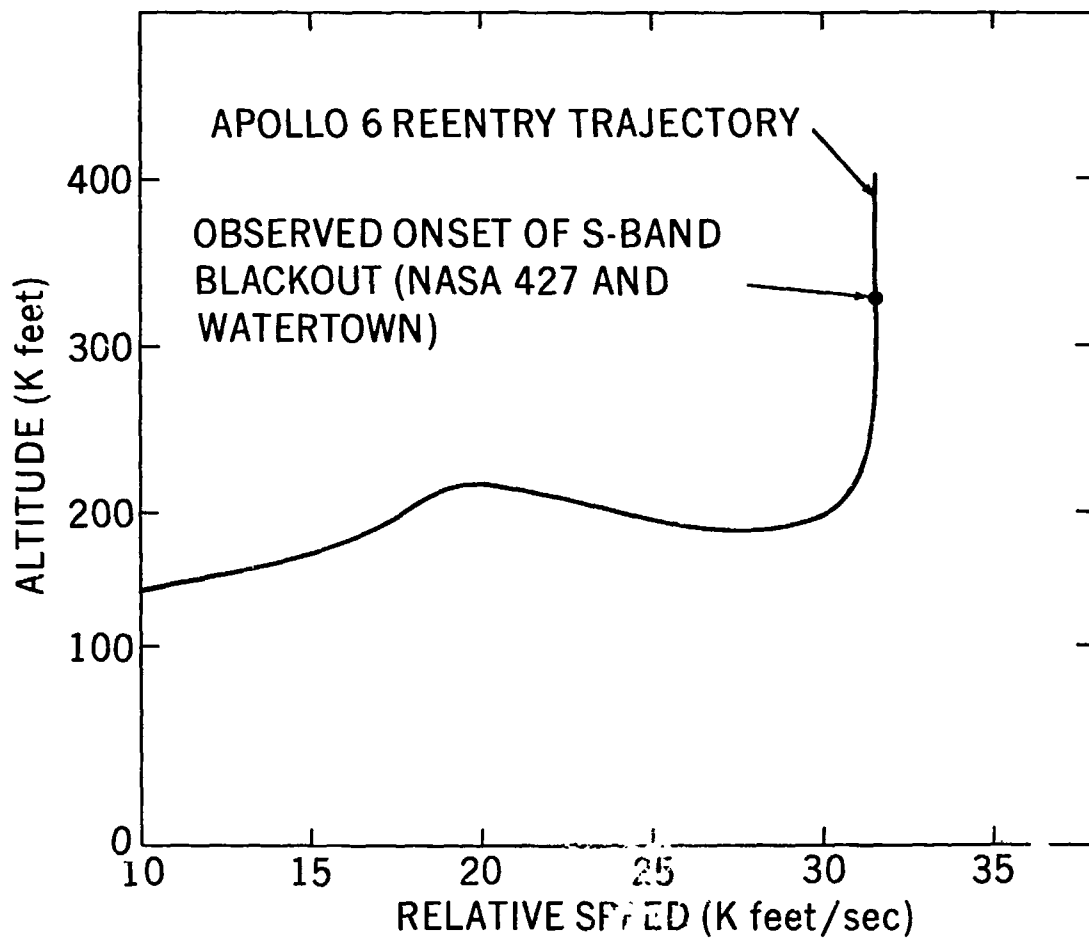
GAIN PLOT (G): POLARIZATION COMPONENT RECORDED UNDER C (1) C (2) C (3) C (4) C (5) C (6) C (7) C (8) C (9) C (10) C (11) C (12) C (13) C (14) C (15) C (16) C (17) C (18) C (19) C (20) C (21) C (22) C (23) C (24) C (25) C (26) C (27) C (28) C (29) C (30) C (31) C (32) C (33) C (34) C (35) C (36) C (37) C (38) C (39) C (40) C (41) C (42) C (43) C (44) C (45) C (46) C (47) C (48) C (49) C (50) C (51) C (52) C (53) C (54) C (55) C (56) C (57) C (58) C (59) C (60) C (61) C (62) C (63) C (64) C (65) C (66) C (67) C (68) C (69) C (70) C (71) C (72) C (73) C (74) C (75) C (76) C (77) C (78) C (79) C (80) C (81) C (82) C (83) C (84) C (85) C (86) C (87) C (88) C (89) C (90) C (91) C (92) C (93) C (94) C (95) C (96) C (97) C (98) C (99) C (100) C (101) C (102) C (103) C (104) C (105) C (106) C (107) C (108) C (109) C (110) C (111) C (112) C (113) C (114) C (115) C (116) C (117) C (118) C (119) C (120) C (121) C (122) C (123) C (124) C (125) C (126) C (127) C (128) C (129) C (130) C (131) C (132) C (133) C (134) C (135) C (136) C (137) C (138) C (139) C (140) C (141) C (142) C (143) C (144) C (145) C (146) C (147) C (148) C (149) C (150) C (151) C (152) C (153) C (154) C (155) C (156) C (157) C (158) C (159) C (160) C (161) C (162) C (163) C (164) C (165) C (166) C (167) C (168) C (169) C (170) C (171) C (172) C (173) C (174) C (175) C (176) C (177) C (178) C (179) C (180) C (181) C (182) C (183) C (184) C (185) C (186) C (187) C (188) C (189) C (190) C (191) C (192) C (193) C (194) C (195) C (196) C (197) C (198) C (199) C (200) C (201) C (202) C (203) C (204) C (205) C (206) C (207) C (208) C (209) C (210) C (211) C (212) C (213) C (214) C (215) C (216) C (217) C (218) C (219) C (220) C (221) C (222) C (223) C (224) C (225) C (226) C (227) C (228) C (229) C (230) C (231) C (232) C (233) C (234) C (235) C (236) C (237) C (238) C (239) C (240) C (241) C (242) C (243) C (244) C (245) C (246) C (247) C (248) C (249) C (250) C (251) C (252) C (253) C (254) C (255) C (256) C (257) C (258) C (259) C (260) C (261) C (262) C (263) C (264) C (265) C (266) C (267) C (268) C (269) C (270) C (271) C (272) C (273) C (274) C (275) C (276) C (277) C (278) C (279) C (280) C (281) C (282) C (283) C (284) C (285) C (286) C (287) C (288) C (289) C (290) C (291) C (292) C (293) C (294) C (295) C (296) C (297) C (298) C (299) C (300) C (301) C (302) C (303) C (304) C (305) C (306) C (307) C (308) C (309) C (310) C (311) C (312) C (313) C (314) C (315) C (316) C (317) C (318) C (319) C (320) C (321) C (322) C (323) C (324) C (325) C (326) C (327) C (328) C (329) C (330) C (331) C (332) C (333) C (334) C (335) C (336) C (337) C (338) C (339) C (340) C (341) C (342) C (343) C (344) C (345) C (346) C (347) C (348) C (349) C (350) C (351) C (352) C (353) C (354) C (355) C (356) C (357) C (358) C (359) C (360) C (361) C (362) C (363) C (364) C (365) C (366) C (367) C (368) C (369) C (370) C (371) C (372) C (373) C (374) C (375) C (376) C (377) C (378) C (379) C (380) C (381) C (382) C (383) C (384) C (385) C (386) C (387) C (388) C (389) C (390) C (391) C (392) C (393) C (394) C (395) C (396) C (397) C (398) C (399) C (400) C (401) C (402) C (403) C (404) C (405) C (406) C (407) C (408) C (409) C (410) C (411) C (412) C (413) C (414) C (415) C (416) C (417) C (418) C (419) C (420) C (421) C (422) C (423) C (424) C (425) C (426) C (427) C (428) C (429) C (430) C (431) C (432) C (433) C (434) C (435) C (436) C (437) C (438) C (439) C (440) C (441) C (442) C (443) C (444) C (445) C (446) C (447) C (448) C (449) C (450) C (451) C (452) C (453) C (454) C (455) C (456) C (457) C (458) C (459) C (460) C (461) C (462) C (463) C (464) C (465) C (466) C (467) C (468) C (469) C (470) C (471) C (472) C (473) C (474) C (475) C (476) C (477) C (478) C (479) C (480) C (481) C (482) C (483) C (484) C (485) C (486) C (487) C (488) C (489) C (490) C (491) C (492) C (493) C (494) C (495) C (496) C (497) C (498) C (499) C (500) C (501) C (502) C (503) C (504) C (505) C (506) C (507) C (508) C (509) C (510) C (511) C (512) C (513) C (514) C (515) C (516) C (517) C (518) C (519) C (520) C (521) C (522) C (523) C (524) C (525) C (526) C (527) C (528) C (529) C (530) C (531) C (532) C (533) C (534) C (535) C (536) C (537) C (538) C (539) C (540) C (541) C (542) C (543) C (544) C (545) C (546) C (547) C (548) C (549) C (550) C (551) C (552) C (553) C (554) C (555) C (556) C (557) C (558) C (559) C (560) C (561) C (562) C (563) C (564) C (565) C (566) C (567) C (568) C (569) C (570) C (571) C (572) C (573) C (574) C (575) C (576) C (577) C (578) C (579) C (580) C (581) C (582) C (583) C (584) C (585) C (586) C (587) C (588) C (589) C (590) C (591) C (592) C (593) C (594) C (595) C (596) C (597) C (598) C (599) C (600) C (601) C (602) C (603) C (604) C (605) C (606) C (607) C (608) C (609) C (610) C (611) C (612) C (613) C (614) C (615) C (616) C (617) C (618) C (619) C (620) C (621) C (622) C (623) C (624) C (625) C (626) C (627) C (628) C (629) C (630) C (631) C (632) C (633) C (634) C (635) C (636) C (637) C (638) C (639) C (640) C (641) C (642) C (643) C (644) C (645) C (646) C (647) C (648) C (649) C (650) C (651) C (652) C (653) C (654) C (655) C (656) C (657) C (658) C (659) C (660) C (661) C (662) C (663) C (664) C (665) C (666) C (667) C (668) C (669) C (670) C (671) C (672) C (673) C (674) C (675) C (676) C (677) C (678) C (679) C (680) C (681) C (682) C (683) C (684) C (685) C (686) C (687) C (688) C (689) C (690) C (691) C (692) C (693) C (694) C (695) C (696) C (697) C (698) C (699) C (700) C (701) C (702) C (703) C (704) C (705) C (706) C (707) C (708) C (709) C (710) C (711) C (712) C (713) C (714) C (715) C (716) C (717) C (718) C (719) C (720) C (721) C (722) C (723) C (724) C (725) C (726) C (727) C (728) C (729) C (730) C (731) C (732) C (733) C (734) C (735) C (736) C (737) C (738) C (739) C (740) C (741) C (742) C (743) C (744) C (745) C (746) C (747) C (748) C (749) C (750) C (751) C (752) C (753) C (754) C (755) C (756) C (757) C (758) C (759) C (760) C (761) C (762) C (763) C (764) C (765) C (766) C (767) C (768) C (769) C (770) C (771) C (772) C (773) C (774) C (775) C (776) C (777) C (778) C (779) C (780) C (781) C (782) C (783) C (784) C (785) C (786) C (787) C (788) C (789) C (790) C (791) C (792) C (793) C (794) C (795) C (796) C (797) C (798) C (799) C (800) C (801) C (802) C (803) C (804) C (805) C (806) C (807) C (808) C (809) C (810) C (811) C (812) C (813) C (814) C (815) C (816) C (817) C (818) C (819) C (820) C (821) C (822) C (823) C (824) C (825) C (826) C (827) C (828) C (829) C (830) C (831) C (832) C (833) C (834) C (835) C (836) C (837) C (838) C (839) C (840) C (841) C (842) C (843) C (844) C (845) C (846) C (847) C (848) C (849) C (850) C (851) C (852) C (853) C (854) C (855) C (856) C (857) C (858) C (859) C (860) C (861) C (862) C (863) C (864) C (865) C (866) C (867) C (868) C (869) C (870) C (871) C (872) C (873) C (874) C (875) C (876) C (877) C (878) C (879) C (880) C (881) C (882) C (883) C (884) C (885) C (886) C (887) C (888) C (889) C (890) C (891) C (892) C (893) C (894) C (895) C (896) C (897) C (898) C (899) C (900) C (901) C (902) C (903) C (904) C (905) C (906) C (907) C (908) C (909) C (910) C (911) C (912) C (913) C (914) C (915) C (916) C (917) C (918) C (919) C (920) C (921) C (922) C (923) C (924) C (925) C (926) C (927) C (928) C (929) C (930) C (931) C (932) C (933) C (934) C (935) C (936) C (937) C (938) C (939) C (940) C (941) C (942) C (943) C (944) C (945) C (946) C (947) C (948) C (949) C (950) C (951) C (952) C (953) C (954) C (955) C (956) C (957) C (958) C (959) C (960) C (961) C (962) C (963) C (964) C (965) C (966) C (967) C (968) C (969) C (970) C (971) C (972) C (973) C (974) C (975) C (976) C (977) C (978) C (979) C (980) C (981) C (982) C (983) C (984) C (985) C (986) C (987) C (988) C (989) C (990) C (991) C (992) C (993) C (994) C (995) C (996) C (997) C (998) C (999) C (1000)

Figure 5. Antenna Pattern of Pair B



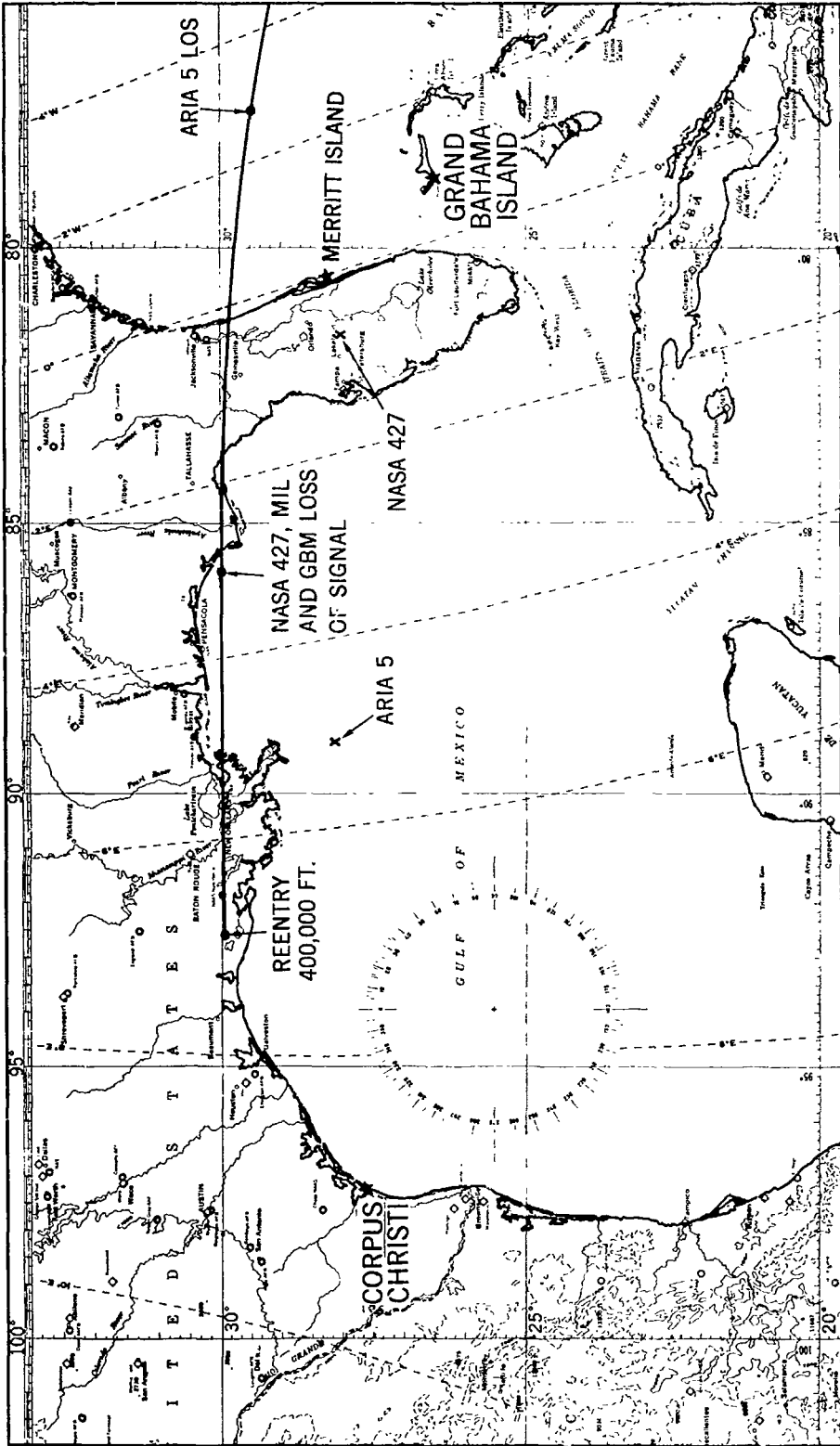
NASA-GSFC-T&DS
MISSION & TRAJECTORY ANALYSIS DIVISION
BRANCH MSAB DATE JUNE 17, 1969
BY MARINI PLOT NO. 1171

Figure 6. Apollo 6 S-Band Signal Strength and Blackout, "Watertown"



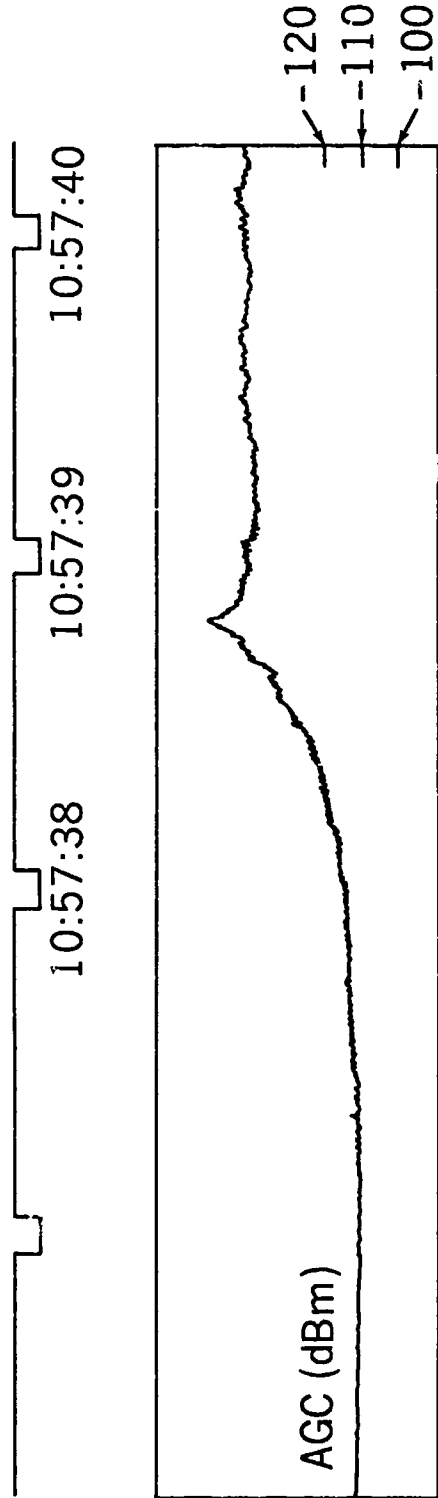
NASA-GSFC-T&DS
MISSION & TRAJECTORY ANALYSIS DIVISION
BRANCH MSAB DATE JUNE 17, 1969
BY MARINI PLOT NO. 1172

Figure 7. Apollo 6 (AS-502) Reentry



NASA-GSFC/EDR
 MISSION & TRAJECTORY ANALYSIS OF APOLLO
 7
 BY: [REDACTED] PLOT NO. [REDACTED]

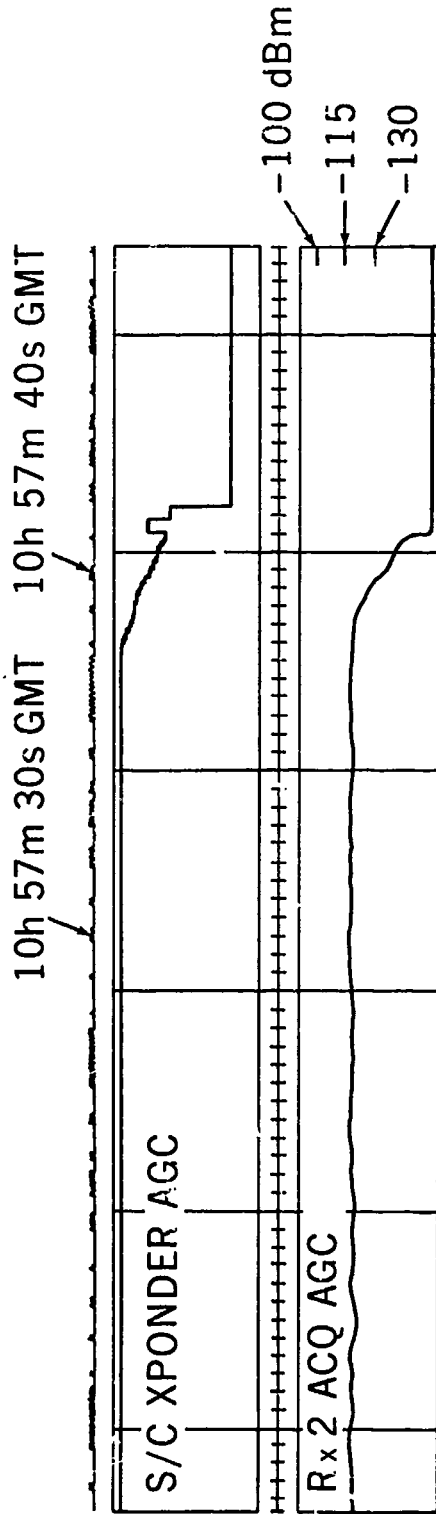
Figure 8. Apollo 7 Reentry Ground Track



NASA-GSFC-T&DS
MISSION & TRAJECTORY ANALYSIS DIVISION
BRANCH MSAB DATE NOV 27, 1968
BY MARINI PLOT NO. 1081

Figure 9. NASA 427 Loss of Signal, Apollo 7 Reentry

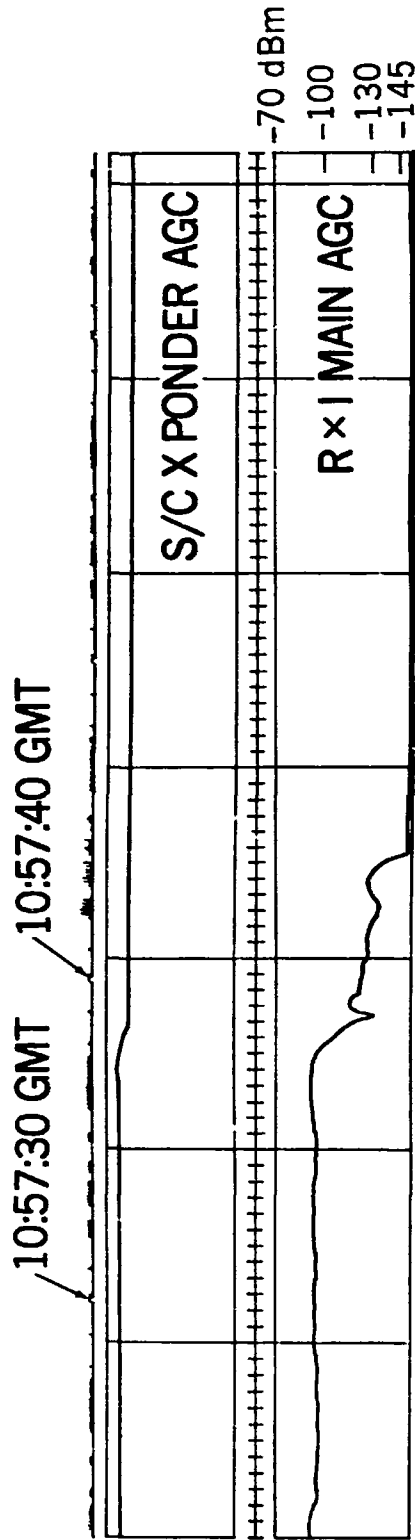
APOLLO FORMAT SERIAL DECIMAL TIME CODE



NASA-GSFC-T&DS
 MISSION & TRAJECTORY ANALYSIS DIVISION
 BRANCH MTAD DATE NOV 27, 1968
 BY MARINI PLOT NO. 1079

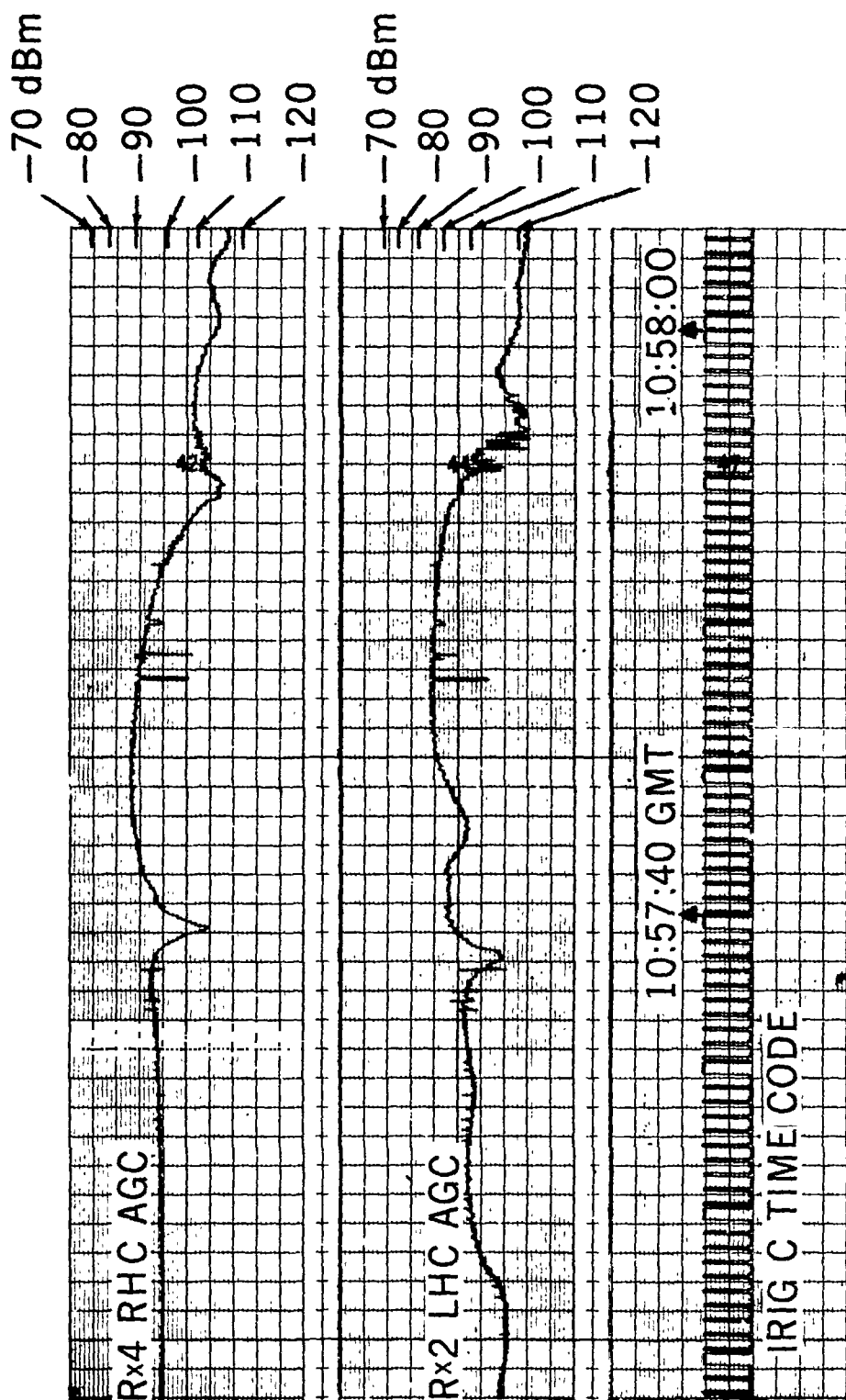
Figure 10. Merrit Island Loss of Signal, Apollo 7 Reentry

APOLLO FORMAT SERIAL DECIMAL TIME CODE



NASA-GSFC-T&DS
MISSION & TRAJECTORY ANALYSIS DIVISION
BRANCH 551 DATE 6-68
BY MARINI PLOT NO. 1173

Figure 11. GBM Loss of Signal, Apollo 7 Reentry

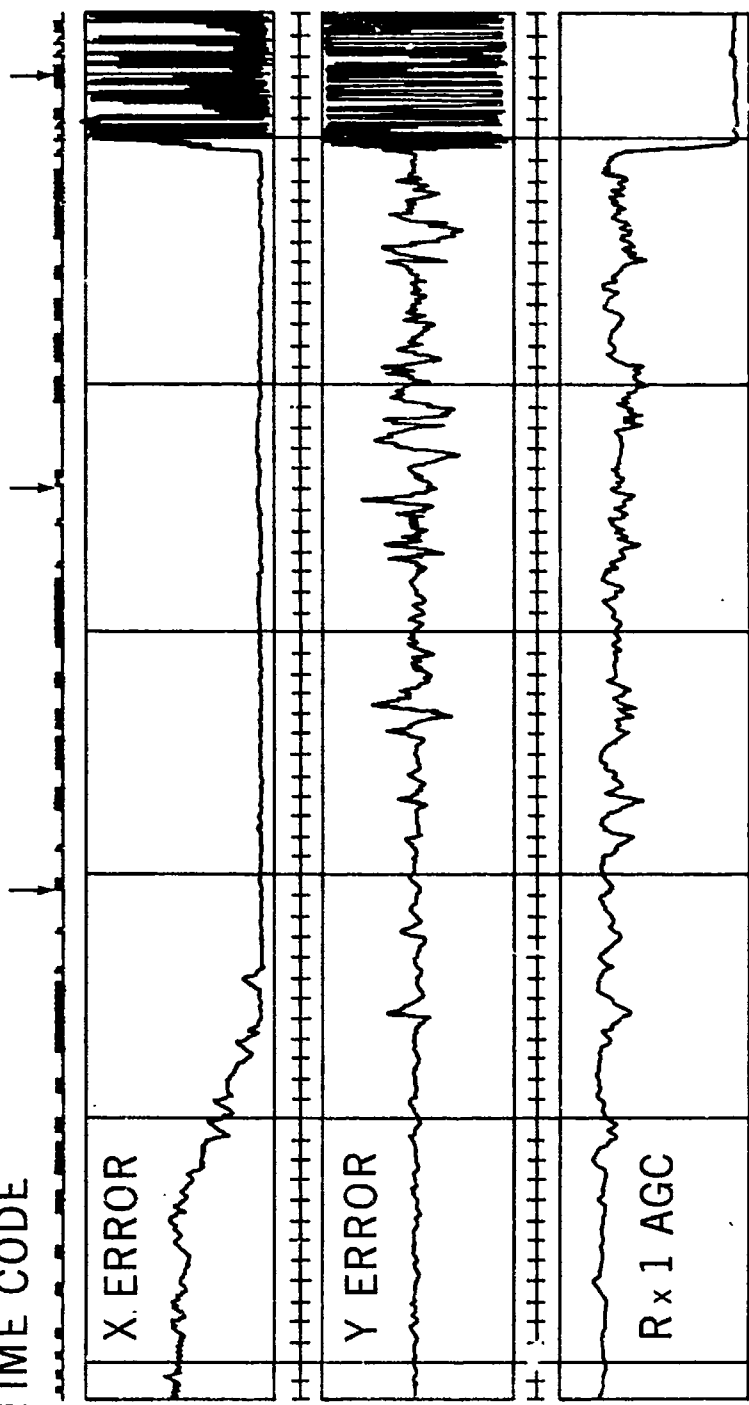


NASA-GSFC-T&DS
MISSION & TRAJECTORY ANALYSIS DIVISION
BRANCH MSAB DATE NOV 27, 1968
BY MARINI PLOT NO. 1084

Figure 12. ARIA 5 AGC, Apollo 7 Reentry

APOLLO FORMAT
 SERIAL DECIMAL
 TIME CODE

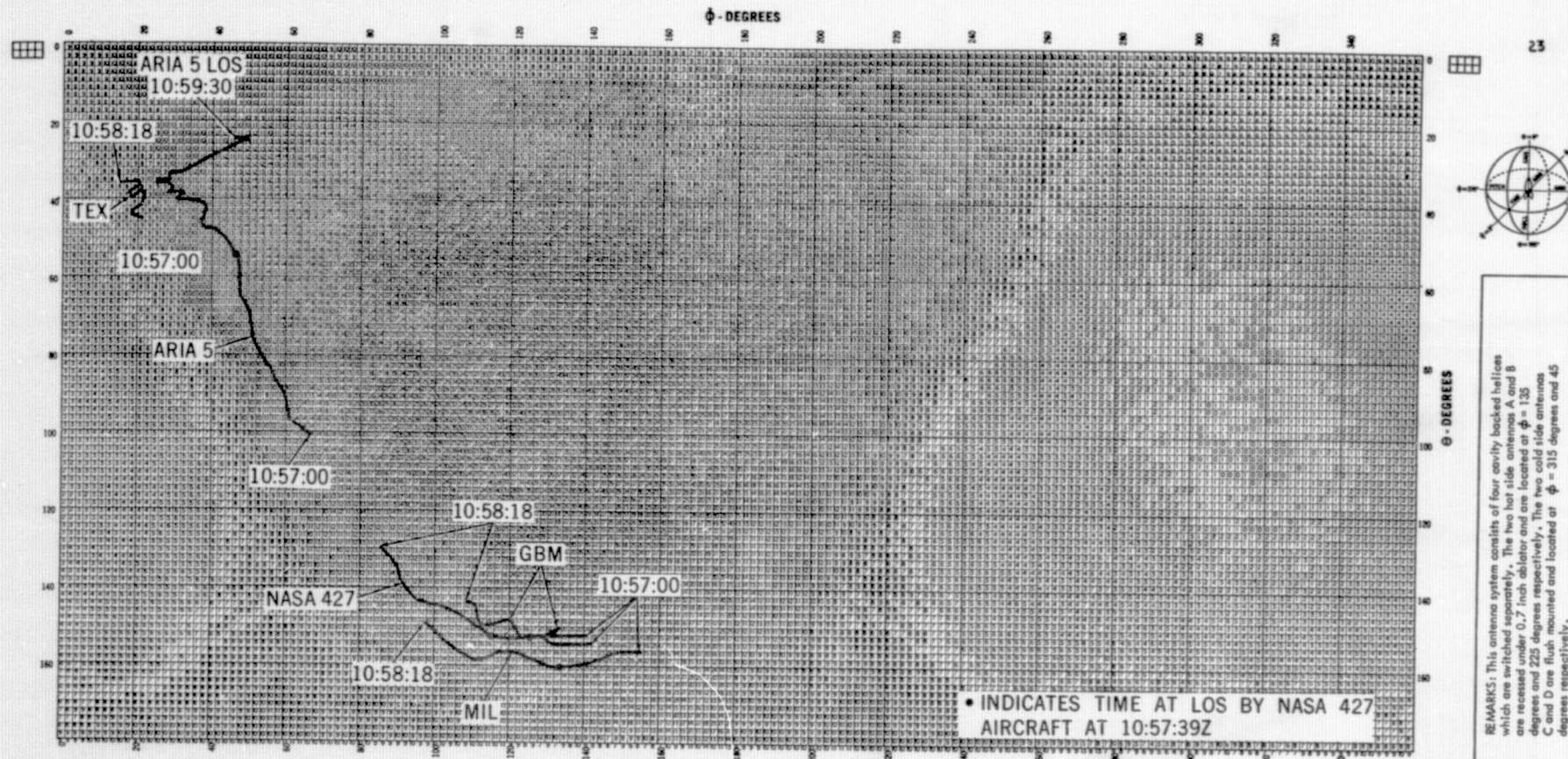
10:57:30 10h 57m 40s GMT 10:57:50



NASA-GSFC-T&DS
 MISSION & TRAJECTORY ANALYSIS DIVISION
 BRANCH MSAB DATE NOV 27, 1968
 BY MARINI PLOT NO. 1082

Figure 13. TEX Loss of Signal, Apollo 7 Reentry

22



REMARKS: This antenna system consists of four empty backed helices which are switched separately. The two hot side antennas A and B are recessed under 0.7 inch ablator and are located at $\phi = 135$ degrees and 225 degrees respectively. The two cold side antennas C and D are flush mounted and located at $\phi = 315$ degrees and 45 degrees respectively.

TEST PROGRAM OR VEHICLE: Block II-QM Only INSTRUMENTATION SYSTEM: MSC Antenna Range PROJECT: Apollo
 DATE: 7-15-67 PATTERN NO.: 9-0 ORGANIZATION: TESD-RSB-Antenna Systems ENGINEER: J. Lindsay
 ANTENNA TYPE: Omni C located at $\phi = 315^\circ$ FREQ. RANGE: S-Band PATTERN MEASUREMENT FREQ: 2287.5 Mc
 PREDOMINANT POLARIZATION: RHC Helix MODEL SCALE: Full LOCATION OF POINT P: (-0.8, 0, 0) -Z Axis

GAIN PLOT: POLARIZATION COMPONENT RECORDED: LINEAR θ ϕ ; CIRCULAR RH LH
 GAINS ARE IN DECIBELS BELOW A REFERENCE LEVEL OF -10 dB ± 0 OR RELATIVE TO AN ISOTROPIC ANTENNA OF RHC POLARIZATION
 PHASE ANGLE PLOT: PHASE ANGLE RECORDED: θ ϕ
 PHASE ANGLES ARE RECORDED VALUES IN DEGREES MULTIPLIED BY 25.

NASA-GSFC-TADS
 MISSION & TRAJECTORY ANALYSIS DIVISION
 BRANCH MSAB DATE NOV 27, 1968
 BY MARINI PLOT NO. 1078

Figure 14. Antenna Gain and Polar Angles to each Station, Apollo 7

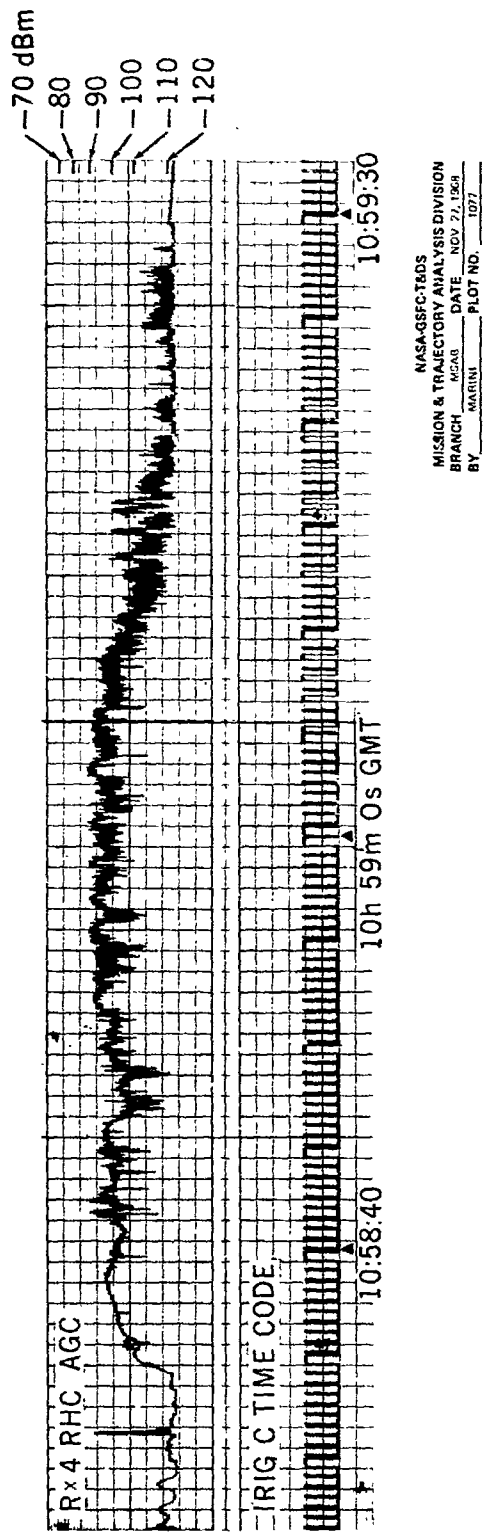
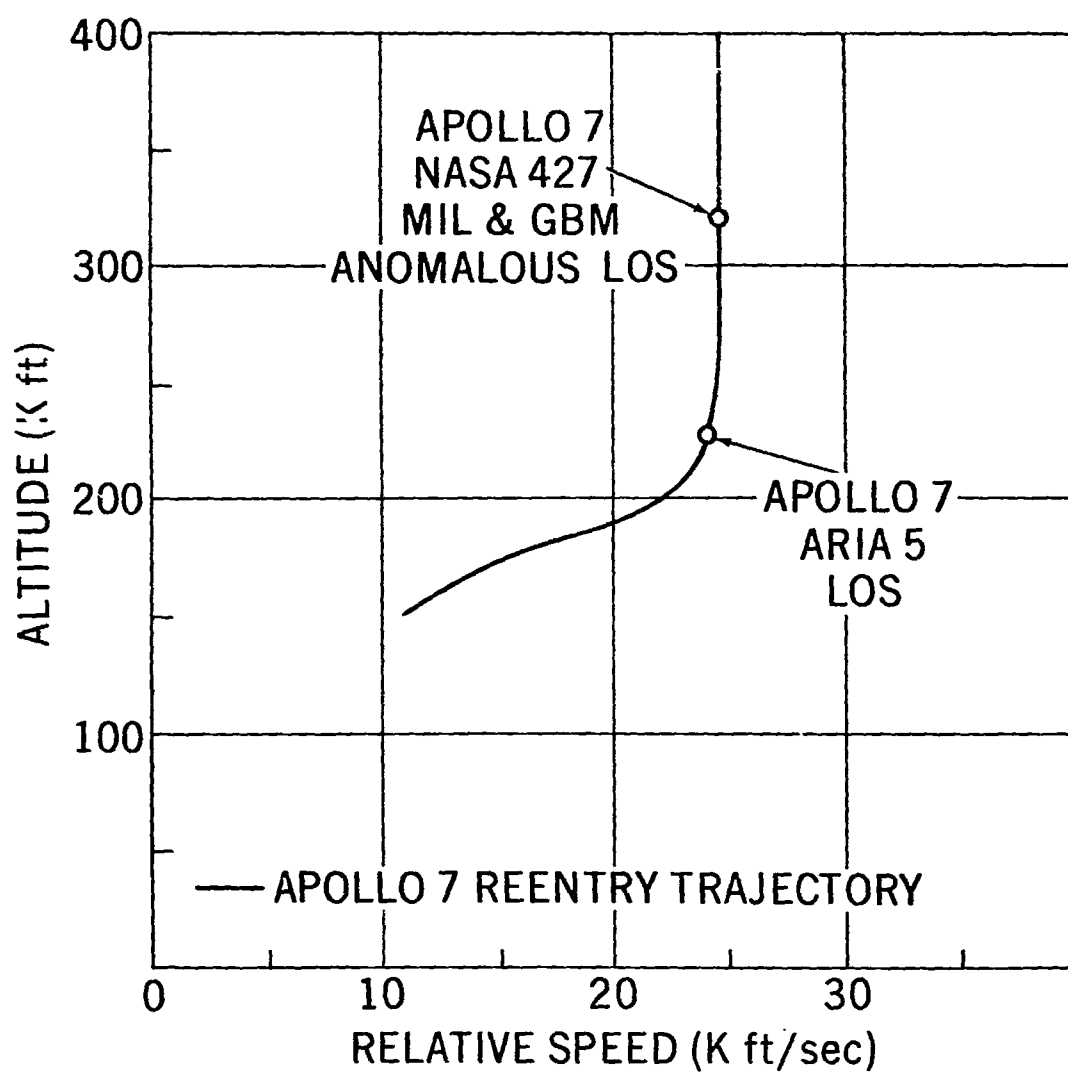
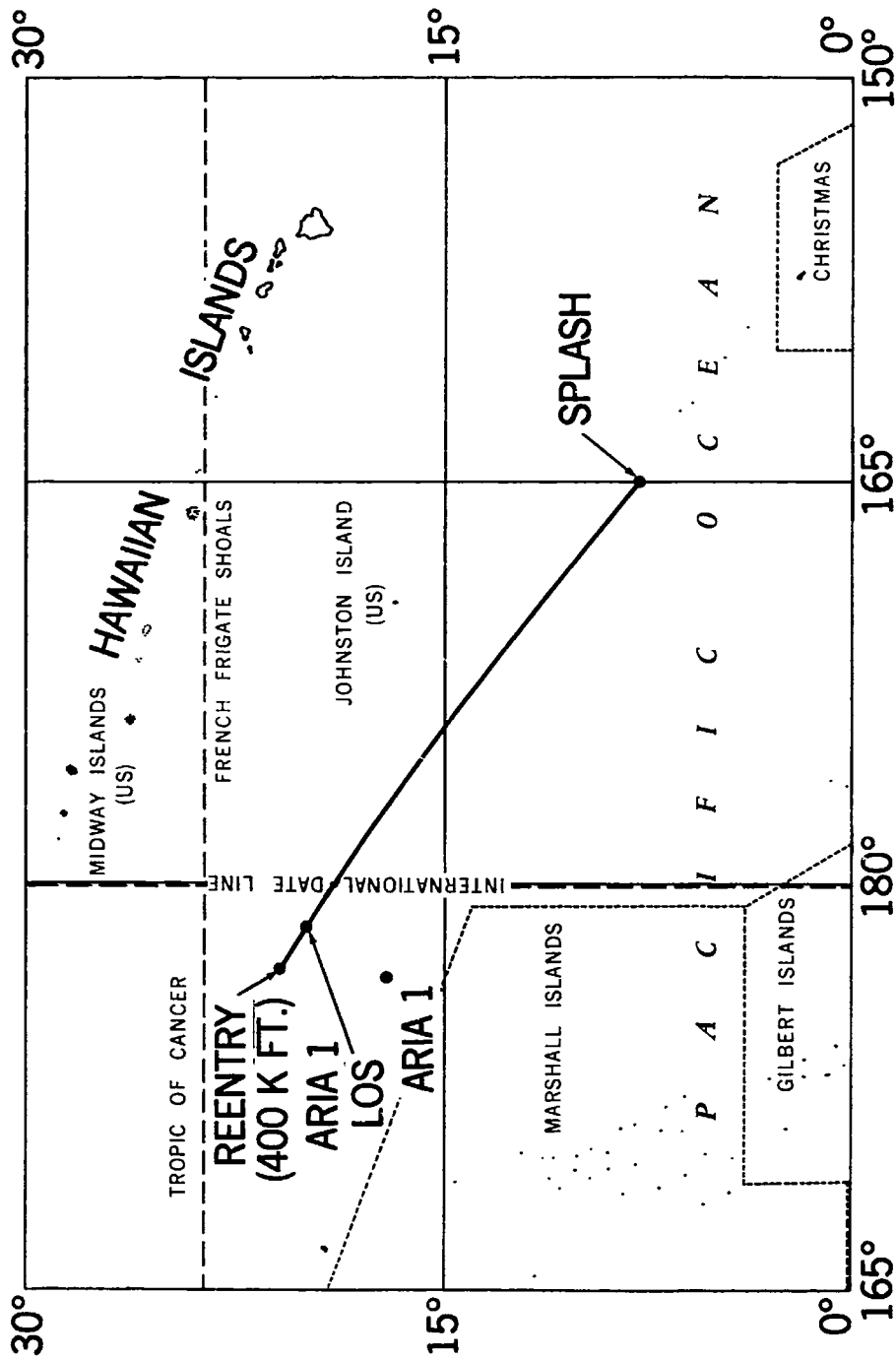


Figure 15. ARIA 5 Loss of Signal, Apollo 7 Reentry



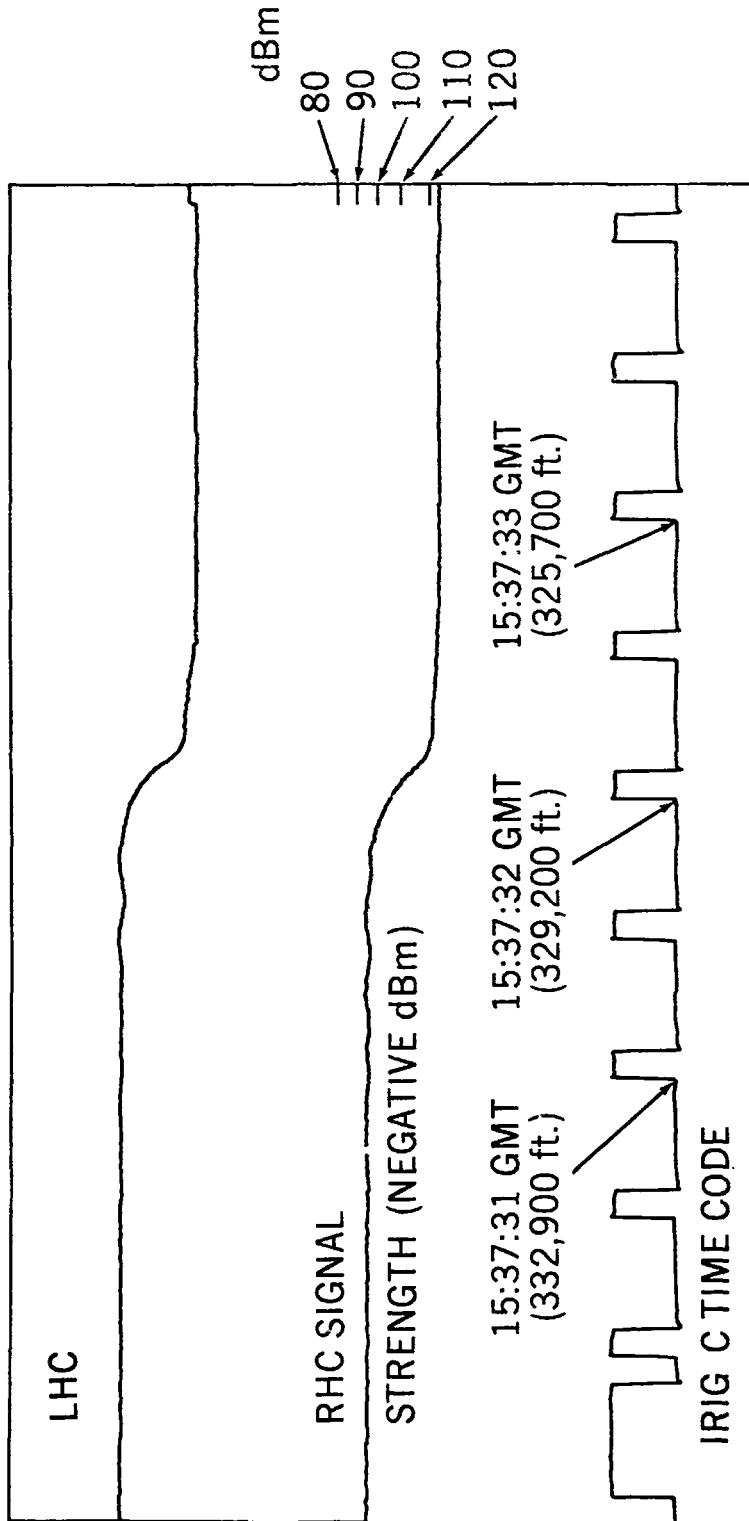
NASA-GSFC-T&DS
MISSION & TRAJECTORY ANALYSIS DIVISION
BRANCH 551 DATE 6-69
BY MARINI PLOT NO. 1174

Figure 16. Apollo 7 Reentry



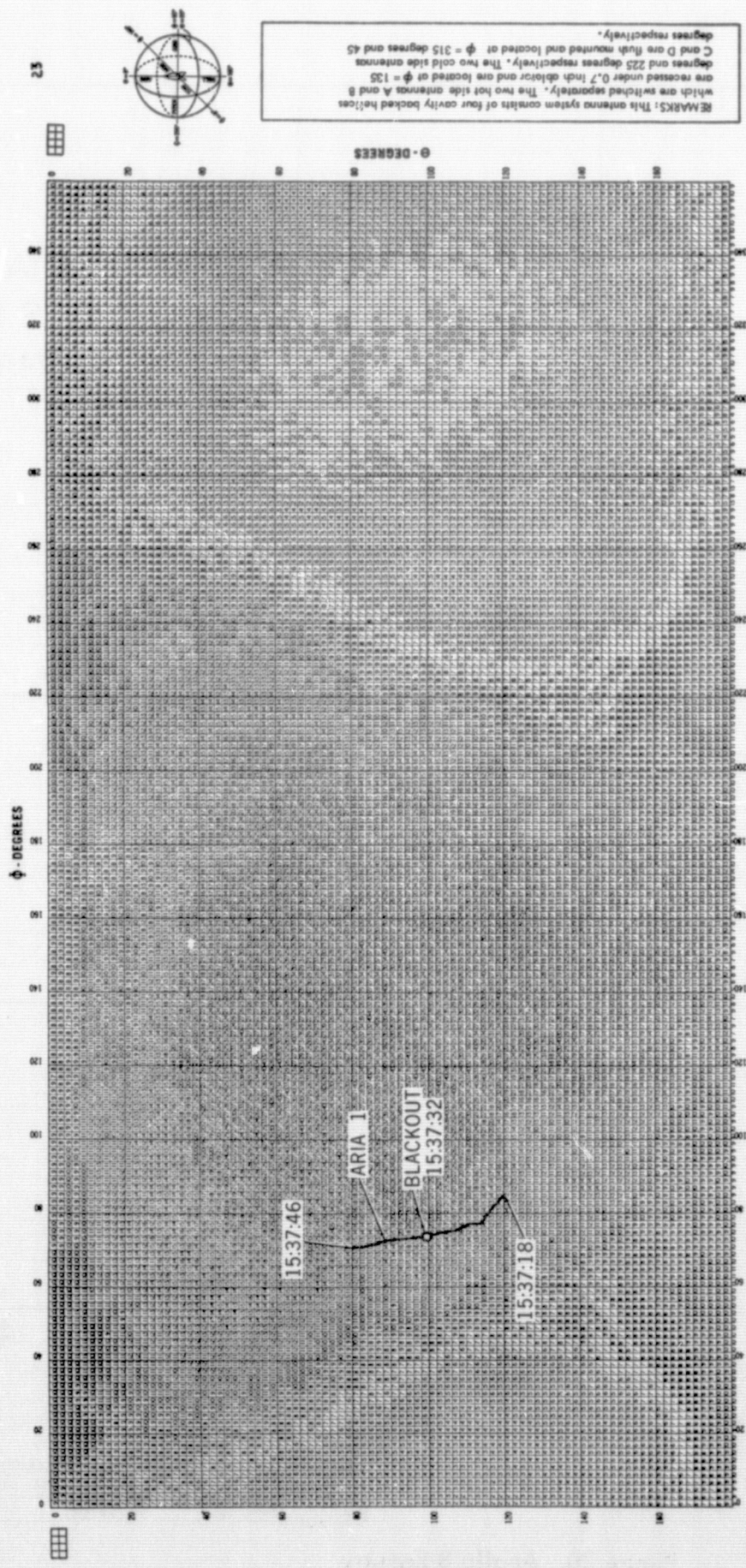
NASA-GSFC-T&DS
MISSION & TRAJECTORY ANALYSIS DIVISION
BRANCH MSAB DATE JUNE 17, 1969
BY MARINI PLOT NO. 1175

Figure 17. Apollo 8 Reentry Ground Track



NASA-GSFC-T&DS
MISSION & TRAJECTORY ANALYSIS DIVISION
BRANCH MSAB DATE JUNE 17, 1969
BY MARINI PLOT NO. 1170

Figure 18. Apollo 8 Blackout, ARIA 1



REMARKS: This antenna system consists of four cavity backed helices which are switched separately. The two hot side antennas A and B are recessed under 0.7 inch obtuse and are located at $\phi = 135$ degrees and 225 degrees respectively. The two cold side antennas C and D are flush mounted and located at $\phi = 315$ degrees and 45 degrees respectively.

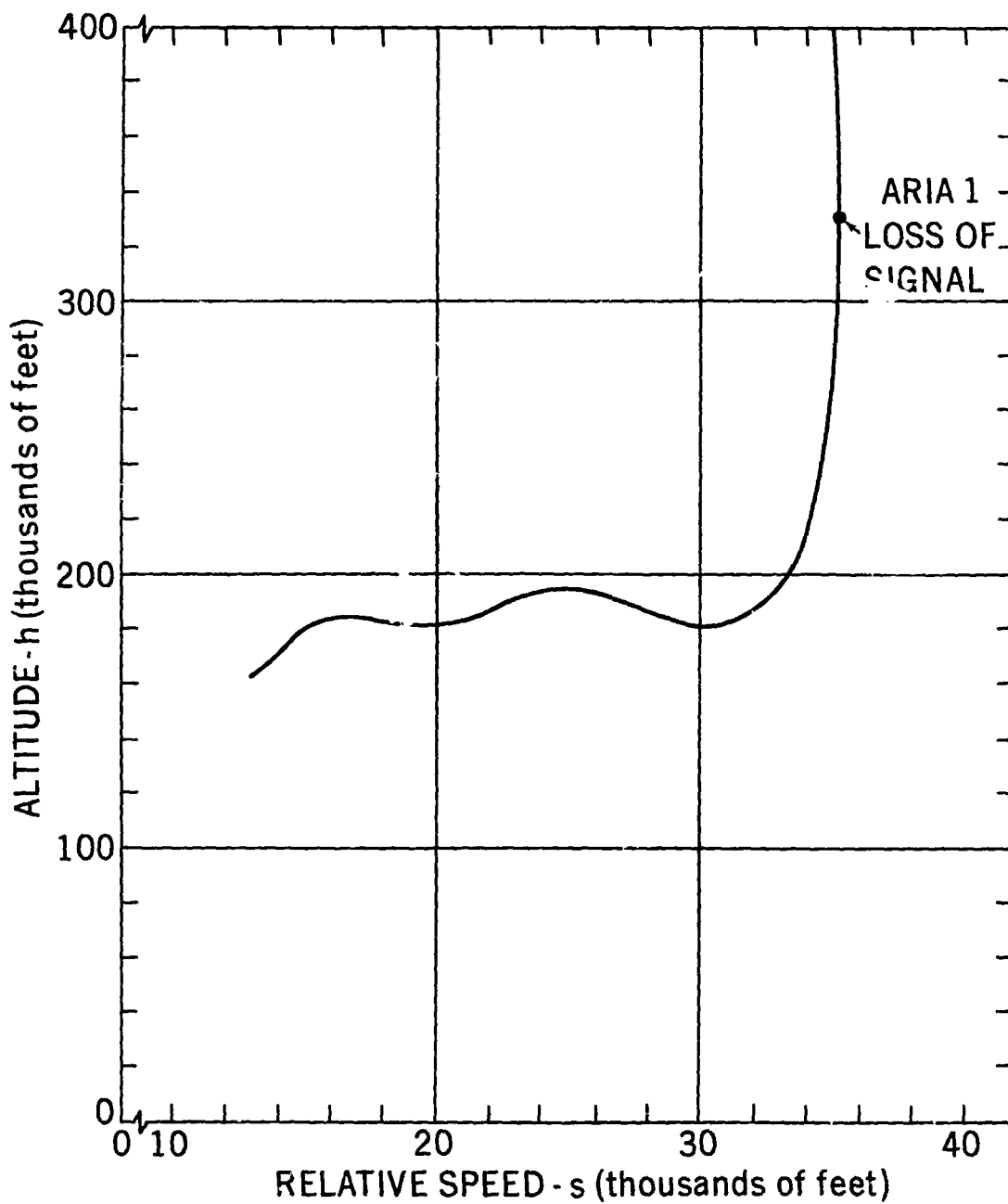
DATA PLOT # POLARIZATION COMPONENT RECORDED LINES C, D, E, F, G, H, I, J, K, L, M, N, O, P, Q, R, S, T, U, V, W, X, Y, Z, AA, AB, AC, AD, AE, AF, AG, AH, AI, AJ, AK, AL, AM, AN, AO, AP, AQ, AR, AS, AT, AU, AV, AW, AX, AY, AZ, BA, BB, BC, BD, BE, BF, BG, BH, BI, BJ, BK, BL, BM, BN, BO, BP, BQ, BR, BS, BT, BU, BV, BW, BX, BY, BZ, CA, CB, CC, CD, CE, CF, CG, CH, CI, CJ, CK, CL, CM, CN, CO, CP, CQ, CR, CS, CT, CU, CV, CW, CX, CY, CZ, DA, DB, DC, DD, DE, DF, DG, DH, DI, DJ, DK, DL, DM, DN, DO, DP, DQ, DR, DS, DT, DU, DV, DW, DX, DY, DZ, EA, EB, EC, ED, EE, EF, EG, EH, EI, EJ, EK, EL, EM, EN, EO, EP, EQ, ER, ES, ET, EU, EV, EW, EX, EY, EZ, FA, FB, FC, FD, FE, FF, FG, FH, FI, FJ, FK, FL, FM, FN, FO, FP, FQ, FR, FS, FT, FU, FV, FW, FX, FY, FZ, GA, GB, GC, GD, GE, GF, GG, GH, GI, GJ, GK, GL, GM, GN, GO, GP, GQ, GR, GS, GT, GU, GV, GW, GX, GY, GZ, HA, HB, HC, HD, HE, HF, HG, HH, HI, HJ, HK, HL, HM, HN, HO, HP, HQ, HR, HS, HT, HU, HV, HW, HX, HY, HZ, IA, IB, IC, ID, IE, IF, IG, IH, II, IJ, IK, IL, IM, IN, IO, IP, IQ, IR, IS, IT, IU, IV, IW, IX, IY, IZ, JA, JB, JC, JD, JE, JF, JG, JH, JI, JJ, JK, JL, JM, JN, JO, JP, JQ, JR, JS, JT, JU, JV, JW, JX, JY, JZ, KA, KB, KC, KD, KE, KF, KG, KH, KI, KJ, KK, KL, KM, KN, KO, KP, KQ, KR, KS, KT, KU, KV, KW, KX, KY, KZ, LA, LB, LC, LD, LE, LF, LG, LH, LI, LJ, LK, LL, LM, LN, LO, LP, LQ, LR, LS, LT, LU, LV, LW, LX, LY, LZ, MA, MB, MC, MD, ME, MF, MG, MH, MI, MJ, MK, ML, MM, MN, MO, MP, MQ, MR, MS, MT, MU, MV, MW, MX, MY, MZ, NA, NB, NC, ND, NE, NF, NG, NH, NI, NJ, NK, NL, NM, NN, NO, NP, NQ, NR, NS, NT, NU, NV, NW, NX, NY, NZ, OA, OB, OC, OD, OE, OF, OG, OH, OI, OJ, OK, OL, OM, ON, OO, OP, OQ, OR, OS, OT, OU, OV, OW, OX, OY, OZ, PA, PB, PC, PD, PE, PF, PG, PH, PI, PJ, PK, PL, PM, PN, PO, PP, PQ, PR, PS, PT, PU, PV, PW, PX, PY, PZ, QA, QB, QC, QD, QE, QF, QG, QH, QI, QJ, QK, QL, QM, QN, QO, QP, QQ, QR, QS, QT, QU, QV, QW, QX, QY, QZ, RA, RB, RC, RD, RE, RF, RG, RH, RI, RJ, RK, RL, RM, RN, RO, RP, RQ, RR, RS, RT, RU, RV, RW, RX, RY, RZ, SA, SB, SC, SD, SE, SF, SG, SH, SI, SJ, SK, SL, SM, SN, SO, SP, SQ, SR, SS, ST, SU, SV, SW, SX, SY, SZ, TA, TB, TC, TD, TE, TF, TG, TH, TI, TJ, TK, TL, TM, TN, TO, TP, TQ, TR, TS, TT, TU, TV, TW, TX, TY, TZ, UA, UB, UC, UD, UE, UF, UG, UH, UI, UJ, UK, UL, UM, UN, UO, UP, UQ, UR, US, UT, UY, UZ, VA, VB, VC, VD, VE, VF, VG, VH, VI, VJ, VK, VL, VM, VN, VO, VP, VQ, VR, VS, VT, VU, VV, VW, VX, VY, VZ, WA, WB, WC, WD, WE, WF, WG, WH, WI, WJ, WK, WL, WM, WN, WO, WP, WQ, WR, WS, WT, WU, WV, WW, WX, WY, WZ, XA, XB, XC, XD, XE, XF, XG, XH, XI, XJ, XK, XL, XM, XN, XO, XP, XQ, XR, XS, XT, XU, XV, XW, XX, XY, XZ, YA, YB, YC, YD, YE, YF, YG, YH, YI, YJ, YK, YL, YM, YN, YO, YP, YQ, YR, YS, YT, YU, YV, YW, YX, YY, YZ, ZA, ZB, ZC, ZD, ZE, ZF, ZG, ZH, ZI, ZJ, ZK, ZL, ZM, ZN, ZO, ZP, ZQ, ZR, ZS, ZT, ZU, ZV, ZW, ZX, ZY, ZZ

DATE PLOT # POLARIZATION COMPONENT RECORDED LINES C, D, E, F, G, H, I, J, K, L, M, N, O, P, Q, R, S, T, U, V, W, X, Y, Z, AA, AB, AC, AD, AE, AF, AG, AH, AI, AJ, AK, AL, AM, AN, AO, AP, AQ, AR, AS, AT, AU, AV, AW, AX, AY, AZ, BA, BB, BC, BD, BE, BF, BG, BH, BI, BJ, BK, BL, BM, BN, BO, BP, BQ, BR, BS, BT, BU, BV, BW, BX, BY, BZ, CA, CB, CC, CD, CE, CF, CG, CH, CI, CJ, CK, CL, CM, CN, CO, CP, CQ, CR, CS, CT, CU, CV, CW, CX, CY, CZ, DA, DB, DC, DD, DE, DF, DG, DH, DI, DJ, DK, DL, DM, DN, DO, DP, DQ, DR, DS, DT, DU, DV, DW, DX, DY, DZ, EA, EB, EC, ED, EE, EF, EG, EH, EI, EJ, EK, EL, EM, EN, EO, EP, EQ, ER, ES, ET, EU, EV, EW, EX, EY, EZ, FA, FB, FC, FD, FE, FF, FG, FH, FI, FJ, FK, FL, FM, FN, FO, FP, FQ, FR, FS, FT, FU, FV, FW, FX, FY, FZ, GA, GB, GC, GD, GE, GF, GG, GH, GI, GJ, GK, GL, GM, GN, GO, GP, GQ, GR, GS, GT, GU, GV, GW, GX, GY, GZ, HA, HB, HC, HD, HE, HF, HG, HH, HI, HJ, HK, HL, HM, HN, HO, HP, HQ, HR, HS, HT, HU, HV, HW, HX, HY, HZ, IA, IB, IC, ID, IE, IF, IG, IH, II, IJ, IK, IL, IM, IN, IO, IP, IQ, IR, IS, IT, IU, IV, IW, IX, IY, IZ, JA, JB, JC, JD, JE, JF, JG, JH, JI, JJ, JK, JL, JM, JN, JO, JP, JQ, JR, JS, JT, JU, JV, JW, JX, JY, JZ, KA, KB, KC, KD, KE, KF, KG, KH, KI, KJ, KK, KL, KM, KN, KO, KP, KQ, KR, KS, KT, KU, KV, KW, KX, KY, KZ, LA, LB, LC, LD, LE, LF, LG, LH, LI, LJ, LK, LL, LM, LN, LO, LP, LQ, LR, LS, LT, LU, LV, LW, LX, LY, LZ, MA, MB, MC, MD, ME, MF, MG, MH, MI, MJ, MK, ML, MM, MN, MO, MP, MQ, MR, MS, MT, MU, MV, MW, MX, MY, MZ, NA, NB, NC, ND, NE, NF, NG, NH, NI, NJ, NK, NL, NM, NN, NO, NP, NQ, NR, NS, NT, NU, NV, NW, NX, NY, NZ, OA, OB, OC, OD, OE, OF, OG, OH, OI, OJ, OK, OL, OM, ON, OO, OP, OQ, OR, OS, OT, OU, OV, OW, OX, OY, OZ, PA, PB, PC, PD, PE, PF, PG, PH, PI, PJ, PK, PL, PM, PN, PO, PP, PQ, PR, PS, PT, PU, PV, PW, PX, PY, PZ, QA, QB, QC, QD, QE, QF, QG, QH, QI, QJ, QK, QL, QM, QN, QO, QP, QQ, QR, QS, QT, QU, QV, QW, QX, QY, QZ, RA, RB, RC, RD, RE, RF, RG, RH, RI, RJ, RK, RL, RM, RN, RO, RP, RQ, RR, RS, RT, RU, RV, RW, RX, RY, RZ, SA, SB, SC, SD, SE, SF, SG, SH, SI, SJ, SK, SL, SM, SN, SO, SP, SQ, SR, SS, ST, SU, SV, SW, SX, SY, SZ, TA, TB, TC, TD, TE, TF, TG, TH, TI, TJ, TK, TL, TM, TN, TO, TP, TQ, TR, TS, TT, TU, TV, TW, TX, TY, TZ, UA, UB, UC, UD, UE, UF, UG, UH, UI, UJ, UK, UL, UM, UN, UO, UP, UQ, UR, US, UT, UY, UZ, VA, VB, VC, VD, VE, VF, VG, VH, VI, VJ, VK, VL, VM, VN, VO, VP, VQ, VR, VS, VT, VU, VV, VW, VX, VY, VZ, WA, WB, WC, WD, WE, WF, WG, WH, WI, WJ, WK, WL, WM, WN, WO, WP, WQ, WR, WS, WT, WU, WV, WW, WX, WY, WZ, XA, XB, XC, XD, XE, XF, XG, XH, XI, XJ, XK, XL, XM, XN, XO, XP, XQ, XR, XS, XT, XU, XV, XW, XX, XY, XZ, YA, YB, YC, YD, YE, YF, YG, YH, YI, YJ, YK, YL, YM, YN, YO, YP, YQ, YR, YS, YT, YU, YV, YW, YX, YY, YZ, ZA, ZB, ZC, ZD, ZE, ZF, ZG, ZH, ZI, ZJ, ZK, ZL, ZM, ZN, ZO, ZP, ZQ, ZR, ZS, ZT, ZU, ZV, ZW, ZX, ZY, ZZ

TEST PROGRAM ON VEHICLE Block II-OK Only INSTRUMENTATION SYSTEM MSE Antenna Range Meter Apollo DATE 7-15-67 ORIGINATOR 1500-850-Atmosphere SYSTEMS ENGINE J. Lindley ANTENNA TYPE Orbital Location at $\phi = 315$ FIELD RANGE 5-3000 PATTERN MEASUREMENT FREQ. 2287.5 MHz FREQUENCY POLARIZATION RHC Full MODEL SCALE FULL LOCATION OF POINT P₁ (8-0, 8-91) -2 AXES

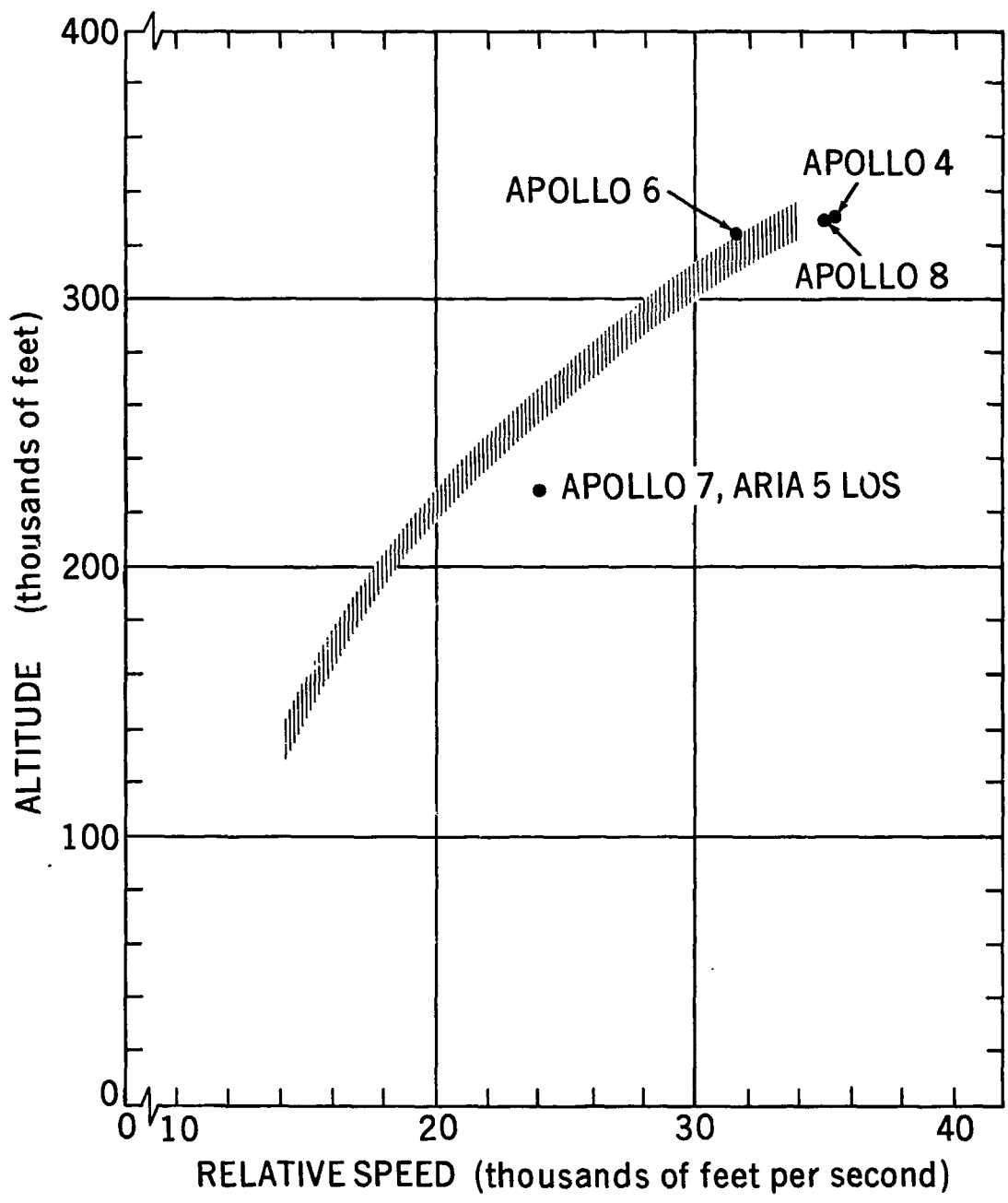
NASA/ASECT/NDOS
MISSION & TRAJECTORY ANALYSIS DIVISION
BRANCH WAFB DATE NOV 27, 1966
BY MARTIN PLOT NO. 1078

Figure 19. Apollo 8 Reentry Antenna Pattern



NASA-GSFC-T&DS
MISSION & TRAJECTORY ANALYSIS DIVISION
BRANCH MSAB DATE JUNE 17, 1969
BY MARINI PLOT NO. 1177

Figure 20. Apollo 8 Reentry



NASA-GSFC-T&DS
MISSION & TRAJECTORY ANALYSIS DIVISION
BRANCH MSAB DATE JUNE 17, 1969
BY MARINI PLOT NO. 1178

Figure 21. Apollo Reentry S-Band Communication Blackout Curve